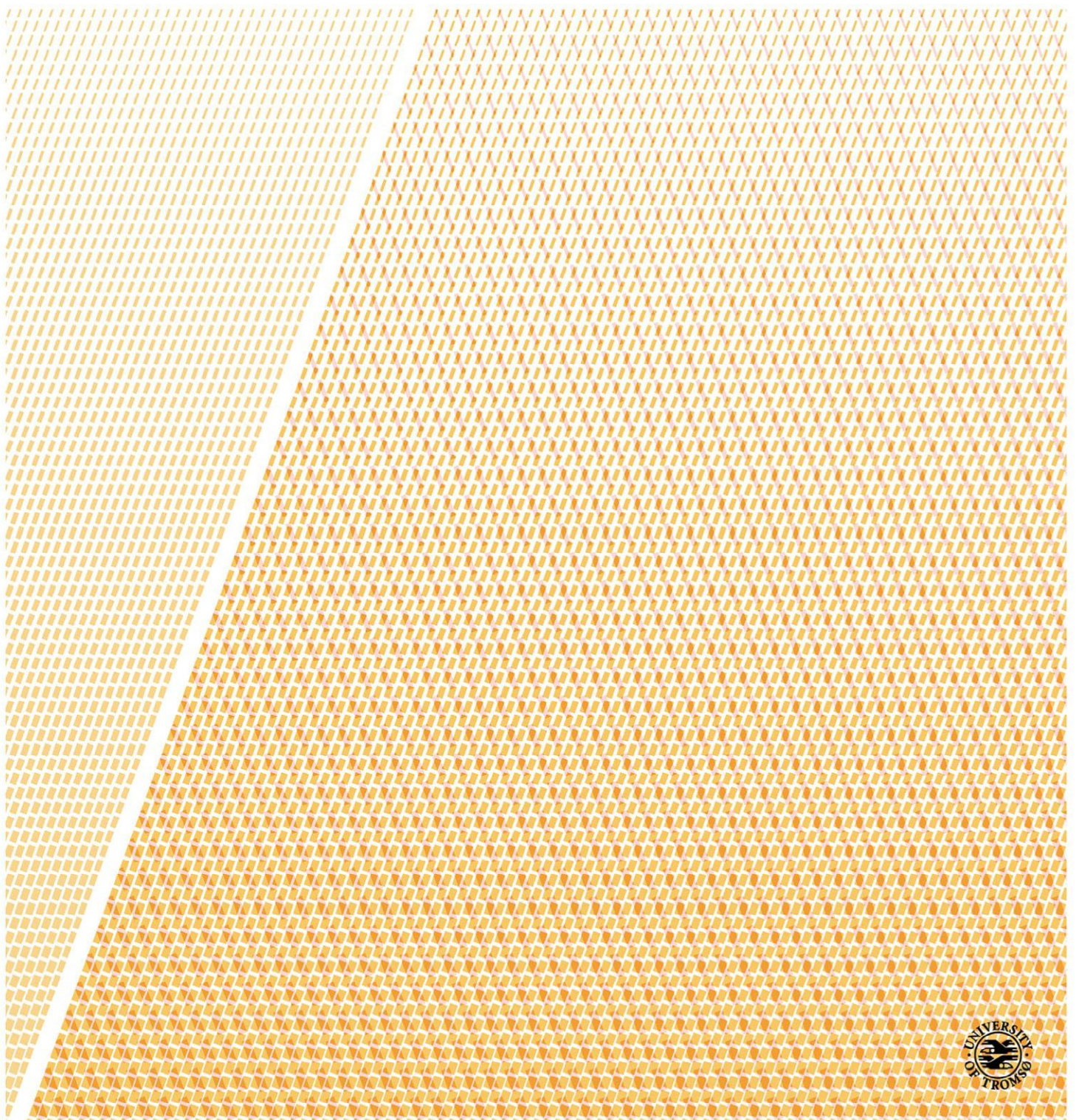Faculty of Science and Technology

Department of Geology

Ice rafting, Ocean circulation and Glacial activity on the western Svalbard margin 0-74 000 years BP
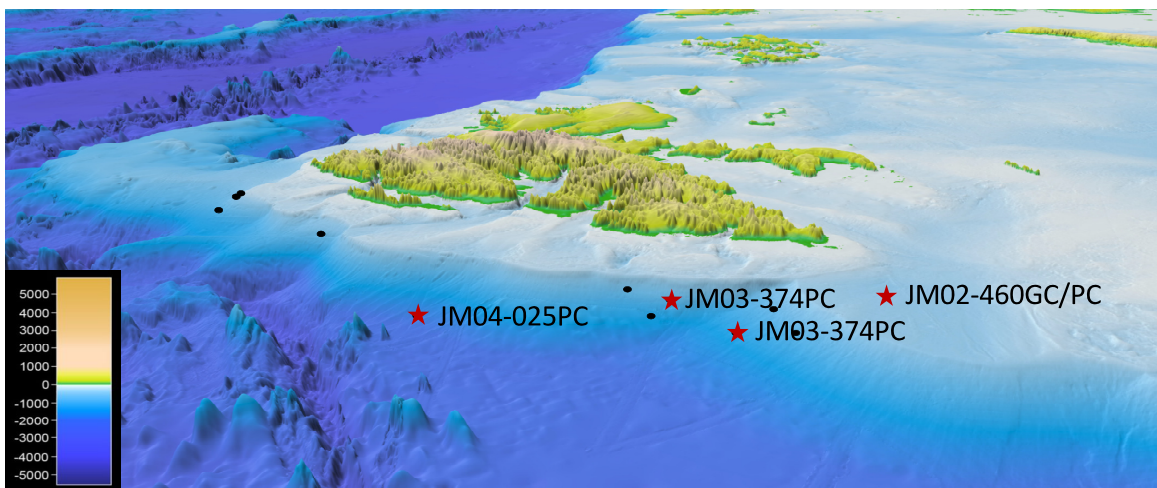
—

Simon Pind Jessen

A dissertation for the degree of Philosophiae Doctor – January 2015

Ice rafting, Ocean circulation and Glacial activity on the western Svalbard margin 0-74 000 years BP

Simon Pind Jessen

Preface

The present thesis is a result of a long academic journey, including seemingly endless de-tours, decoys and dead-ends. Long lasting struggles is the acid-test for patience. My own, my family's, my supervisor's (and the administration's) has certainly been put to the test - and beyond, more than once.

The thesis mainly builds upon cores from three education- and research cruises by the University Centre in Svalbard (UNIS) with R/V Jan Mayen (now R/V Helmer Hanssen) to the western Svalbard margin in may 2003, 2004 and 2005. I participated in 2003 as geology student and oceanography responsible, in 2004 as teacher within geology and oceanography. The possibility to use magnetic susceptibility and lithology for a new chronology (presented in Paper I) was initially discovered during the cruise in 2003, when we retrieved three cores from three different locations from the western Svalbard slope all showing the same patterns. During the 2004 cruise, we expected to find the same patterns again. And so we did. Since then, the patterns continue to show up in cores from coring stations along the western Svalbard slope. A more life directing discovery for me also happened in 2003 in Svalbard, when I met my wife, Kristine. Along with the research my family has been growing steadily into three kids, Toke, Tana and Maya (and the same amount of parental leave prolonging the thesis writing process).

Parallel to the thesis work I have worked with science communication and public outreach and teaching in the course GEO3111 all fall semesters 2006-2013 as assistant for the exercises and as main teacher in 2007, 2008 and 2013. The principal public outreach was done as part of the International Polar Year project, SciencePub. My contribution was to be the main responsible for the marine geological part of Quaternary geology exhibition aimed at 8th-10th graders. This was done along with my colleagues Steffen Aagaard-Sørensen and Kasia Zamelzcyk, (both now researchers at the Department of Geology in Tromsø). I have also been responsible for welcoming visiting high school classes to the department and secretary for the local Tromsø part of the national research school in climate dynamics ResClim.

Acknowledgements

The laboratory staff in Tromsø (Trine Dahl and Ingvild Hald) has assisted with sampling, sieving and some measurements (mainly on the Sedigraph 5100) together with Nikoline L. Rasmussen and Julia Sen.

Matthias Forwick, with whom I shared an office for quite a few years is thanked for several inputs on data interpretation and graphical presentation. I have received encouragement from both Matthias and the late Tore Ola Vorren during my work with the thesis. Matthias is now head of the department, and it is sort of fitting that it is under his charge, I - finally - deliver.

Our now retired graphical magician, Jan P. Holm, has helped with several plots and maps, both for the thesis work and my outreach projects. Thank you, and happy retirement!

To Nils Martin Hanken. Thanks a lot for interesting discussions in the laboratory and corridors on the minerals, flora, fauna and concretions showing up in my cores.

Jan Sverre Laberg reviewed Paper III. Your comments are most appreciated.

In general I want to acknowledge my fellow Ph. D. candidates, the students, Post Docs., the permanent staff and the administration for a good and enjoyable working atmosphere (that is everybody, I guess). Also I want to explicitly mention all my students having followed GEO3111 and critically assessed my results and ideas during lectures and laboratory work.

The captains and crews of R/V Jan Mayen (R/V Helmer Hanssen) are acknowledged for retrieving the interesting sediment cores during a series of cruises. Some of the cores are presented here. And for making the life at sea as pleasant as possible for us visiting scientists (also when the waves are getting high).

Students and scientists joining the UNIS marine geology cruises in 2003 − 2006 are acknowledged for their contribution in retrieving the cores.

Professor Ian Snowball introduced me to magnetic susceptibility during a course in 2003 at UNIS, Svalbard. He participated in the UNIS cruise in 2003, where we first discovered the repeated magnetic susceptibility pattern that are now the basis of Paper I in the present thesis. He analyzed cores for paleo-intensity, which has helped establishing a chronology reaching further back than the 30,000 years in Paper I. Also he hosted me during a two-month stay at Lund University Paleomagnetic Laboratory, summer 2010.

Tove Nielsen Co-authored Paper I and was cruise responsible in 2005 and 2006. And also contributed by interesting discussions throughout 2004-6 when she was the main marine geologist at Unis.

Anders Solheim Co-authored Paper I and was in charge of the seismic part of the cruises responsible in 2003 – 2005. Most of the coring stations were chosen from his seismic lines.

To everyone in Honningsvåg at 71°N: Thank you for your warm welcome to my family, when we moved here in august 2014. To re-use a quotation one of my home countries comedians, we actually moved to Honningsvåg by mistake. The mistake being that we did not move here long before.

To my supervisor Tine Rasmussen. Apart from letting me use unpublished data, teach a lot of wonderful students and taking up the seemingly impossible challenge of guiding me towards the end of a Ph. D. project, here I mainly want to thank you for not losing confidence in me even when I did myself.

Table of Contents

List of Papers

Paper I

Jessen, S.P., T. L. Rasmussen, T. Nielsen, and A. Solheim (2010), A new Late Weichselian and Holocene marine chronology for the western Svalbard slope 30,000–0 cal years BP, *Quaternary Science Reviews* 29, 1301–1312.

Paper II

Jessen, S.P., and T. L. Rasmussen *(submitted)*, Sortable Silt Cycles in Svalbard Slope Sediments 74-0 ka, *Submitted to Journal of Quaternary Science, submission no. JQS-15-0006.*

Paper III

Jessen, S. P., and T. L. Rasmussen, Ice rafting patterns on the western Svalbard slope 74–0 ka: Interplay between ice sheet activity and ocean circulation, *Manuscript to be submitted to Paleoceanography*

Paper IV

Rasmussen, T. L., E. Thomsen, M. A. Ślubowska, S. P. Jessen, A. Solheim, and N. Koç (2007), Paleoceanographic evolution of the SW Svalbard margin (76°N) since 20,000 ^{14}C yr BP, *Quaternary Research* 67, 100–114.

Author contribution Paper IV

Simon P. Jessen contributed with the counting of Ice Rafted Detritus in the core JM03-373PC and discussions on data interpretation, and commenting on late versions of the manuscript.

1. Motivation and approaches

The main focus of the present thesis is the interplay between climate, ocean circulation and ice sheet activity during the last 74,000 years. Glaciers and ice sheets plays a significant role in climate, oceanography and sea level change. Previously glaciated areas can serve as natural laboratories for studies of the dynamic of ice sheets and glaciers. The Scandinavian landscape is shaped by the action of ice sheets and the sediments on the shelves and slope off Norway, the Barents Sea and Svalbard are mainly deposited by ice and melt water (e.g., Lundqvist, 1986; Houmark-Nielsen, 1999; Mangerud, 2004). Both the geomorphology within previously glaciated areas and the sediments deposited outside previously glaciated areas can provide evidence of the dynamics of the glacial ice on time scales of up to millions of years.

1.1. Choice of study area and main focus

In the present thesis the interaction between climate, ocean and ice sheets on centennial, millennial and orbital time scales is described and discussed (Papers I and III). The ice sheet is the Svalbard-Barents Sea Ice Sheet and the study area is the western Svalbard margin (Figure 1). This area offers a unique natural, high Arctic laboratory for the study of ocean-climate-ice sheet interactions. The western Svalbard margin is located close to the edge of a large former ice sheet. Today, the presence of Atlantic water at the surface provides generally sea ice free conditions year-round, which offers relatively easy accessibility for research vessels. The sedimentation rate is generally sufficient for high-resolution reconstructions of environmental conditions on centennial and decadal scales (Eiken and Hinz, 1993). Another very interesting feature of the Svalbard-Barents Sea Ice Sheet is that it was mainly grounded below present-day sea level (e.g., Elverhøi and Solheim, 1983; Landvik et al., 1998; Siegert and Dowdeswell, 2002, 2004; Svendsen et al., 2004). This makes the Svalbard-Barents Sea Ice Sheet the best paleo-analogue to the probably most climate sensitive large ice mass on earth today, the West Antarctic Ice Sheet (e.g., Winsborrow et al., 2010).

1.2. Approaches

1.2.1. Reconstructing glacial history based on sediment cores from the adjacent slope

The extent, advance and retreat of the former Svalbard-Barents Sea Ice Sheet have been subjected to more than 150 years of research (reviewed by Ingólfsson and Landvik, 2013). The PONAM project in the 1990's (Elverhøi et al., 1998) provide a very solid foundation for further assessing the history and dynamics of the ice sheet. This thesis is based

on marine core records from the western Svalbard slope. According to Jon Landvik (pers. comm.) the study of slope sediments is a kind of "remote sensing" of the behavior of an ice sheet. A lot of good reasons can be listed for assessing an ice sheet from a remote location. The general gain from the study of marine records contra in-situ studies from within the previously glaciated area is a continuous and more detailed chronology and a broader overview. In-situ evidence of one glaciations-deglaciation cycle is often overprinted by younger events, since glaciers and ice sheets are destructive by nature, in-situ studies are often strongly affected by the latest glacial action (e.g., Elverhøi and Solheim, 1983; Landvik et al., 2013; Ingólfsson and Landvik, 2013). Evidence once archived outside the glaciated area has a better chance of surviving the next glaciations and the sediments eroded from a glaciated area and accumulated outside the glaciated area serve as handy 'remote' archives for several glaciations-deglaciation cycles (e.g. Elverhøi et al., 1995; Andersen et al., 1996; Mangerud et al., 1998; Vogt et al., 2001). Ocean sediments have to some extent proven easier to date than terrestrial records based on oxygen isotope stratigraphy and ^{14}C dates (bearing in mind the problems of variations in the marine reservoir effect and sometimes the lack of datable material (e.g., Bondevik et al., 2006; Polyak et al., 2008; Reimer et al., 2013). Ocean sediment cores can provide a context for the glacial history with regards to changes in climate and oceanography since the sediment cores often include possible climate proxies in addition to information of the glacial movements (e.g., Bond et al., 1992, 1993; Rasmussen et al., 1996; van Kreveld et al., 2000; Vogt et al., 2001) (Paper I, III, IV). In addition, a study area that has been in direct contact with a big ice sheet is more likely to include significant hiatuses, since an inactive ice sheet can block the area from receiving sediments and because an active ice sheet is erosive. The possibility for hiatuses is also a potential problem in marine records (some of the cores presented in this thesis include hiatuses).

Even though it is possible to list a lot of good arguments for using marine cores as "remote sensors" for glacial activity, of course studying ice sheets from a marine record has down sides too. A very important cost of a remote location is loss of details. Slope sediments will only record the glacial activities that lead to sedimentation on the slope. This means mainly the actions going on at the nearest rim of the ice sheet. The dynamics and processes of the interior of the ice sheet can only be assessed in-situ. As for all kinds of 'remote sensing' a solid ground truthing is needed to interpret the glacial history and dynamics meaningfully from marine ocean cores. The geomorphology of the Barents Sea has now been studied in detail for more than a decade by 3D seismic and swath bathymetry surveys (Ottesen et al., 2005, 2007; Andreassen et al., 2008; Winsborrow et al., 2010). These have proven that the

bed shapes of the Barents Sea are largely formed by the actions of the ice sheet at its maximum, and by the actions of the retreating ice sheet (Andreassen et al., 2008; Rüther et al., 2011). Together with dated terrestrial studies of geomorphology and latest ice exposure points to a much more dynamic deglaciation than previously acknowledged for Svalbard and the Barents Sea, with series of glacial retreat phases, still stands and possibly re-advances (Landvik et al., 2005; Alexanderson et al., 2011; Gjermundsen et al., 2013; Hormes et al., 2013; Landvik et al., 2014). The absolute timing of glacial retreats, still stands and re-advances is still unknown, since the marine acoustic surveys lack absolute age control. A joint-venture between "in-situ" and "remote sensing" paleo-studies is the more effective way to improve our basal understanding of glacier-ocean-climate interactions (e.g., Hormes et al., 2013; Alexanderson et al, 2014).

1.2.2. Reconstructing bottom current strength from a sediment record

The thesis also targets the variations in bottom current activity over the western Svalbard slope through the last 74,000 years. Several studies from the western Svalbard margin and the Fram Strait has focussed on the reconstruction of paleoceanography i.e., the presence and properties of specific water masses in the past (e.g., Jones and Keigwin, 1988; Hebbeln et al., 1994; Dokken and Hald, 1996; Hald et al., 2001; Nørgaard-Pedersen et al., 2003; Zamelczyk et al., 2013) (Paper IV). A main contribution of Paper IV is paleo-temperature profiles for the western Svalbard slope at 76 °N (Paper IV, Figure 8), and the documentation of continuous presence of Atlantic water on the western Svalbard slope also during cold intervals. Several studies also uses benthic foraminifera as bottom current indicators, mainly the species *Cibicidoides wuellerstorfi* or *Cibicides lobatulus* (e.g., Haake and Pflaumann, 1989; Rasmussen et al., 1996b; Ślubowska et al., 2005, Ślubowska-Woldengen et al., 2007, Skirbekk et al., 2010; Rasmussen and Thomsen, 2015) (Paper IV). In Paper II we have studied the past variations in bottom current activity on millennial scale based on sortable silt and magnetic susceptibility and to some extent presence of C. *wuellerstorfi*. In Paper I, magnetic susceptibility is suggested to partly reflect changes in bottom current strength as also indicated in studies from the SE Nordic seas and North Atlantic (e.g., Rasmussen et al., 1996a; Moros et al., 1997; Kissel et al., 1999).

1.3. Objectives

The main objectives of the thesis are:

1.   To improve the late Weichselian chronology of sedimentary records form the western Svalbard slope and to reconstruct the paleoceanography,

2.   To reconstruct dynamics of the Svalbard-Barents Sea ice sheet on orbital and millennial time scale, and

3.   To reconstruct bottom current strength on the western Svalbard slope on millennial and orbital time scales.

2. Study area

2.1. Sedimentary environments

The western Svalbard slope generally consists of late Pliocene to Quaternary sediments characterised by a series of glacigenic Trough-Mouth Fans and inter-fan areas overlying the bedrock. The fan and interfan areas contain the same sediment facies (Faleide et al., 1996; Solheim et al., 1998). The Trough-Mouth Fans are mainly built by a series of mass transported sediments deposited during full glacial conditions (Laberg and Vorren 1995, 1996; Hjelstuen et al., 1996; Vorren et al., 1998) (Paper I). Thinner mass transport deposits are also found in the inter-fan areas (e.g., Andersen et al, 1996; Solheim et al., 1998) (Paper I). Both the fan and inter-fan areas are draped with hemipelagic sediments (e.g., Andersen et al., 1996; Dokken and Hald, 1996; Hald et al., 2004; Howe et al., 2008) (Papers I–IV). For at least 3 million years, bottom current activity has generated contourite deposits along the western and northern Svalbard margin at 1000–3000 m water depth (Eiken and Hinz, 1993). Packages of laminated fine-grained sediments were deposited during deglaciations and are generally interpreted as a result of fast ice retreat from intensified melting (Andersen et al., 1996; Vogt et al., 2001; Pedrosa et al., 2011; Lucchi et al., 2013) (Papers I, III and IV). Another possibility is sudden releases of water from sub-glacial lakes (Svendsen et al., 2004).

2.2. Oceanography

The upper 500–700 meters of the water column consist of warm Atlantic Water transported in the West Spitsbergen Current overlying cold (T ~ -1 °C) intermediate and deep water generated from convection in the Nordic Seas (e.g., Aagaard et al., 1985; Hopkins, 1991). The mean flow on the western Svalbard slope is northwards (e.g., Hopkins, 1991;

Osiński et al., 2003; Walczowski et al., 2005). The flow of the West Spitsbergen Currents is steered topographically over the slope (e.g., Rudels, 1987; Hopkins 1991). The flow strength is strongest over the 800 to 2000 meter isobaths, where velocities in July 2000 and 2002 reached 40–55 cm/s in the upper 150 meter of the water column centred over the 1200 m isobath (Osiński et al., 2003). The warmest (>7 °C in July 2002) and most saline (>35.1 in July 2002) part of the Atlantic water is centred over the 800 m isobath (Osiński et al., 2003). Direct current measurements show northward transport of Atlantic water along the slope of approximately 6 to 14 Sv (1 Sv = 1 Sverdrup = $1*10^6$ m^3/s) (Aagaard et al., 1973; Fahrbach et al., 2001; Osiński et al., 2003; Schauer et al., 2004; Walczowski et al., 2005; Marnela et al., 2008). The main part of the Atlantic Water recirculates and flows to the south below the cold East Greenland Current (e.g., Quadfasel et al., 1987; Rudels et al., 2000; Eldevik et al., 2009). The net inflow of Atlantic water to the Arctic Ocean via the Fram Strait is c. 1 Sverdrup (Grotefendt et al., 1998).

3. Ice Rafted Detritus – a seemingly simple proxy

This thesis mainly investigates sediments and the composition of the sediment with great emphasis on the content of Ice Rafted Detritus (IRD). Other proxies used are grain-sizes of sortable silt and magnetic susceptibility, stable isotopes (δ^{18}O, δ^{13}C) and microfossils. IRD in marine records is generally defined as mineral grains of sand size (e.g., Ruddiman, 1977; Andrews, 2000; Bischof, 2000). All four papers of this thesis include IRD records. In Paper III, IRD is the center of attention (e.g., see Heinrich, 1988; Bond et al., 1993, 1997, 1999; Bond and Lotti, 1995; Andersen et al., 1996; Andrews, 2000; Bischof, 2000; Moros et al., 2004; Rørvik et al., 2010). In Paper I, the main focus is on magnetic susceptibility and lithology together with the content of IRD and the distribution of stable isotopes measured in planktic foraminifera. In Paper II, IRD is treated as a potential problem for the interpretation of sortable silt, 10–63 μm. In Paper IV, IRD is used as an additional proxy along with a thorough fauna study.

3.1. The simple study of IRD

The underlying concept of IRD is attractively simple. Sand-size sediments are too heavy for current transportation by the generally modest ocean currents (e.g., Ruddiman,

1977; Bond et al., 1993; Andrews, 2000). Thus, if coarse grains appear in deep ocean sediments, they must have been transported there. If down slope mass wasting can be ruled out, transportation by icebergs or sea ice is the only reasonable option.

It is also attractively simple to quantify the distribution patterns of IRD (e.g., Andrews, 2000). The work-load can be very small compared to for instance a study based on microfossils. The technical part of an IRD study consists of counting of mineral sand grains in a self-defined grain-size fraction (e.g., Grobe, 1987; Heinrich, 1988; Bond et al., 1992, 1993; Andrews, 2000) (Papers I and IV). Or - as done in several studies - the weighing of a certain self-defined grain-size fraction (e.g., Grobe, 1987; Hass, 2002; Aagaard-Sørensen et al., 2010) (Paper II). However, a record of distribution of IRD is probably easy to obtain, but the interpretation can be anything but simple as shown below.

3.2. The complex interpretation of IRD

3.2.1. Theoretical problems

The process of bringing IRD out to sea and into ocean sediments at a specific study area is basically a function of three main parameters: 1. The release of sediment-rich ice into the ocean, 2. Transportation of the ice to or away from the study area and 3. The melting of ice at the core site (i.e. dependent of surface water temperature on-site) (e.g., Watkins et al., 1974; Smythe et al., 1985; Matsumoto, 1996; Bond et al., 1999). Thus, an IRD record is the final product of a potentially long 'production line' involving iceberg production, sediment entrainment in glacier ice, surface currents, subsurface currents, sea ice production, sediment entrainment in sea ice, sea ice drift, surface water temperatures and subsurface water temperatures - both at the coring site and along the route from ice source to the site (Andrews, 2000) (Figure 2b). A change in any of the above mentioned parameters can result in changes in the concentration or flux of IRD and the composition of the IRD. An IRD record alone can have several possible and probable explanations, which is why IRD is a proxy that cannot stand alone. To make sense of an IRD study, both the study methodology and environmental settings need to be taken into account.

High concentration or flux of IRD is often interpreted as an indicator for calving of icebergs to the ocean. If the coring station is located near a previously glaciated margin, IRD is most often used as a proxy for calving of local icebergs from the local ice sheet (e.g., Paper I, IV). However, this seemingly straightforward interpretation can be an over-simplification. Cores located directly under recently disintegrated ice shelves on the Antarctic Peninsula contain long transported IRD from foreign sources, 'allochthonous' IRD (Pudsey and Evans,

2001). Thus, without distinguishing between local and allochthonous IRD, an IRD increase in a record can give a false impression of a more actively calving local ice sheet. IRD can also be lacking from a sample for several reasons. It may be a probable explanation that no or very little ice passed the station, but also the station could also have been passed by 'clean' ice deprived of sediments large enough to be classified as IRD. Or ice melting at the site could be very limited due to very cold surface and subsurface water.

3.2.1.1. Temperature effects on ice rafting

Russel-Head (1980) offers an equation for the melt-rate of ice in water as a function of temperature (Figure 2a). According to this equation, the melting potential of Atlantic Water west of Svalbard with temperatures of typically 2–5°C (e.g., Aagaard et al., 1985; Hopkins, 1991, Walczowski et al., 2005) is 1 to 2 orders of magnitude higher than the melting potential of Polar Water <-1°C.

Since ice melt faster with increasing temperatures, the IRD flux is positively correlated with the surface and subsurface water temperature directly at the coring station (the temperature 'on-site') (Figure 2b). Conversely the IRD-flux is negatively correlated with the (sub)surface water temperature along the route between the ice source(s) and the core location (the temperature 'en route'). A decrease in temperature 'en route' will increase the amount of ice that can reach a given core site. At low latitudes ice will normally melt before reaching the site, but if the climate gets cold enough, IRD can still travel a long distance. During North Atlantic Heinrich Events the melt water from melted icebergs "paved" a route for the icebergs to cross the North Atlantic from the Laurentide Ice Sheet and reach to southern Portugal (d'Errico and Sanchez Goñi, 2003), The well dated, high-resolution core MD99-2331 west of northern Portugal, show that during Heinrich event H4, H2 and H1, the IRD is deposited later than the initial drop in sea surface temperature (Naugthon et al., 2007, 2009). This indicates that cold surface water had to be in place before ice could survive the journey from North America to Portugal. At high latitudes the melting potential of ocean water may be very important for IRD deposition (cf. McIntyre et al., 1972; Ruddiman and McIntyre, 1981; Smythe et al., 1985). The water surrounding icebergs and sea ice can be too cold to melt the ice and IRD deposition would be very limited regardless of the amount of ice and sediments passing a coring site. Cold surface water may, however, be accompanied with a warmer subsurface water mass, as e.g., in the Arctic Ocean today. Should an iceberg of a few hundred m's thickness be released into the Arctic Ocean its lower part would reach the submerged

Atlantic water layer and melt relatively fast while smaller icebergs and sea ice would hardly melt at all.

3.2.1.2. Climatic effects on glacier dynamics and the sediment in icebergs

Temperature also has a clear effect on glacial dynamics and thereby on the incorporation of sediment. The sediment incorporation with a glacier bed above the pressure melting point, 'temperate ice', is an order of magnitude higher than in ice frozen to the ground, 'cold ice' (e.g., Alley and MacAyeal, 1994; Elverhøi et al., 1998). The temperature regime of an ice sheet depends on the geothermal heat flux, the regional temperature, and the thickness of the ice (e.g., MacAyeal, 1993b). The thicker the ice sheet, the higher is the likelihood for the ice to be temperate, both because of a higher pressure lowering the melting point and because of the insolation effect. It is not only the incorporation of sediments into the ice that is influenced by the glacial setting. Also the possibility for sediments to drop out prior to iceberg calving can be affected. Icebergs calving from the front of ice shelves are often 'clean' compared to icebergs calving from tide water glaciers, because a significant amount of sediment has dropped out from the floating ice shelf prior to calving (e.g., Dowdeswell and Murray, 1990; Domack et al., 1998). Icebergs and sea ice trapped in land fast sea ice may similarly release sediments, while being trapped (Andrews, 2000). Build-up of ice shelves, icebergs being trapped in land fast sea ice and very low melt rates in the ocean are mainly attributed to cold climate. Thus a reduced flux of IRD can also reflect climatic cooling.

3.2.1.3. Ocean temperature effects on the mineral composition of IRD

The mineral composition of IRD is independent of the water temperature 'on-site' and should only reflect the geology of the source area(s) and show the provenance of IRD (e.g., Bond et al., 1993, 1997, 1999; Bond and Lotti, 1995). However, ocean temperature changes can affect IRD provenance and the mineral composition in IRD. The water temperature 'en route' determines the possibility for sand grains from different sources to reach a specific core site (cf. Smythe et al., 1985; Bond et al., 1992) (section 3.2.1.1). In general, warmer surface water 'en route' favors the deposition of IRD from nearby sources (local IRD), because the ice melts faster and may disappear before reaching far from its source (Figure 2c). Colder surface water 'en route' conversely allows the ice to travel longer distances before melting completely. Accordingly, colder surface water 'en route' will increase the extent of potential source areas of IRD for any core site, and thereby favor the deposition of allochthonous IRD (Figure 2d).

3.2.2. Practical problems

3.2.2.1. Size matters

Scientists tend to study IRD in different grain-size fractions and very often in only one grain-size fraction (e.g., Papers I, II). Basically all sizes of sand and gravel have been used as a definition of IRD in the literature. From very fine grained sand, >63 μm (Hass, 2002; Birgel and Hass, 2004) or 63–150 μm (Bond and Lotti, 1995; Bond et al., 1997), over fine sand 150–250 μm (e.g., Werner et al., 2013), >150 μm (e.g., Bond et al. 1993, 1997; Rasmussen et al., 1996a), >180 μm (Heinrich, 1988), medium size sand grains >250 μm (e.g., Bischof, 2000; Knutz et al., 2002a,b; Bauch et al., 2012), over coarse sand >500 μm (e.g., Skirbekk et al., 2010) and very coarse sand >1 mm (e.g., Rørvik et al., 2010) to gravel >2–32 mm (e.g., Grobe, 1987; Andersen et al., 1996; Rørvik et al., 2010). Some studies have used different grain-size fractions for different cores (e.g., Darby and Zimmermann, 2008) (Paper IV). When referring to previously published IRD records the used grain-size of IRD is often not mentioned. The reasoning behind the very varying definition of IRD is the assumption that IRD results are not significantly influenced by the chosen grain-size (e.g., Ruddiman, 1977). However, studies including more than one grain-size fraction in the same core have shown that this assumption is not always valid. IRD counts from the same samples in different grain-size fractions are not always as well correlated as they should be, if IRD counts were grain-size independent (e.g., Andrews, 2000; Weltje and Prins, 2003, 2007) (Paper III). For core JM03-374PC, the shared variation of IRD concentration >150 μm and IRD concentration >500 μm is less than 50% (r^2=0.49) (Figure 3a). Also for the core JM04-025PC (Paper III, Figure 8a) and JM03-373PC (not shown), the shared variation of IRD 150–500 μm and IRD >500 μm is in the order of c. 50%. The correlation between IRD >150 μm and IRD >250 μm in JM04-374PC is better, but still the r^2 is only slightly above 0.6 (Figure 3b). The correlation between IRD >250 μm and IRD >500 μm on the other hand is good with an r^2 of 0.87 μm (Figure 3c). The comparison of IRD counts in different grain-size fractions in JM03-374PC suggests that fine-grained IRD and coarse-grained IRD on the western Svalbard slope are affected by different transport mechanisms (Paper III).

Also the outcome of a study of the mineral composition of IRD will be grain-size dependent. In core JM03-374PC, the content of mono-crystalline quartz grains in the same samples are c. 15–20%-points higher in the fraction 150–250 μm than in the fraction >250 μm (Figure 3d) (Jessen, 2005). In general, a higher relative content of quartz can be expected

when the grain-size is fine, since quartz is chemically stable it is very hard and durable. Thus, less stable minerals will erode and weather faster than quarts and in general, weathering can cause dominance of quartz by removing other minerals. Though higher quartz content in the finer grain-size fraction is consistent, the shared variation of the two data series of % quartz is not very high (64%, Figure 3e) supporting that different transport mechanisms can work on fine-grained and coarse-grained IRD. In general, there are two very unlike types of ice that can deliver sediments to the ocean, icebergs and sea ice. Bischof and Darby (1997) observed a discrepancy between the inferred source of IRD >250 μm and IRD 45–250 μm for the same samples in cores from the interior of the Arctic Ocean. They suggest that a large proportion of the fraction 45–250 μm is sea ice rafted. The sediment incorporation into Arctic sea ice occurs in or adjacent to high energy environments as beaches, rivers and shallow water shelves (Kempema et al., 1989). Sea ice IRD can also be expected to include more rounded grains than iceberg rafted IRD (e.g., Stickley et al., 2009; Forwick and Vorren, 2009). On average, sea ice rafted IRD consist of finer grains than iceberg rafted IRD (e.g., Bischof et al., 2000; Weltje and Prins, 2003, 2007; Darby and Zimmermann, 2008).

3.2.2.2. Weighing or counting?

Andrews (2000) counted IRD in the size fraction >2 mm in a core from the Labrador Sea. The size fraction was also weighed. The two methods gave quite different results. Counting and weighing similarly gives different results for the core JM03-373PC from 1485 m water depth on the Storfjorden fan (Figure 1) (Papers I,II and IV). An IRD count of grains >150 μm, is only partly correlated with the wt% of the residue >150 μm with r^2 of 0.43 (Figure 4b). For the coarser grain-size fraction >500 μm, the comparison of weights and counts of IRD is even more problematic. The samples show a bi-modal distribution (Figure 4a), and thus cannot be correlated. Samples from JM03-373PC may be meaningfully grouped according to the IRD counts and the wt% >500 μm, but to use wt% of coarse grained sand as a proxy for IRD for the whole core would not work very well. The finer grained fraction 150–500 μm show a much better correlation between IRD counts and wt% of the fraction. r^2 reaches 0.76 (Figure 4c), so for relatively fine-grained IRD the wt% seem to work reasonably well as an IRD proxy on the western Svalbard slope, at least for this core.

3.2.2.3. Choice of method and size fraction

The choice of method and grain-size fraction often depends on the abundance of IRD and also the purpose of the study and how much time the scientist(s) can allocate to counting the IRD. To determine the presence or concentration of IRD, a relatively coarse fraction with only a few grains pr sample might be sufficient (e.g., Grobe, 1987). For a petrological study of mineral composition, at least 300 individual grains is needed in each sample to obtain reasonable statistics (e.g., Bond and Lotti, 1995; Bond et al., 1997). To obtain at least 300 grains it is often necessary to choose a relatively fine-grained fraction. Some classical IRD studies from the middle of the North Atlantic has determined IRD concentration from count of IRD >180 μm (Heinrich, 1988) and >150 μm (Bond et al., 1992, 1993, 1997, Bond and Lotti, 1995). To study mineral composition, Bond and Lotti (1995) and Bond et al. (1997) had to use the finer grain-size fraction 63–150 μm. If a core is located very near an active ice stream or a previously active paleo-ice stream a much coarser fraction can allow a mineral composition study. Rørvik et al. (2010) studied a core located near the Vestfjorden Ice Stream, which was very active during the last glacial maximum c. 25–17 ka. In this study, the IRD fraction >1 mm contained enough grains for quantification of the composition of the IRD.

3.3. Making sense of IRD data – a summary

An IRD record cannot stand alone. IRD concentration, flux or mineral composition needs to be interpreted in combination with other proxies to gain information about regional climatic and environmental changes. Either by proxies for water temperature and salinity, preferably from the same core, and/or correlation with other studies from the study area. Including both fine-grained and coarse-grained IRD can enhance the insight to the processes involved in sand grain transportation (e.g., Bischof and Darby, 1997; Andrews, 2000) (Paper III). When comparing different records of IRD, the setting of the study area, the choice of method and the grain-size fraction defined as IRD should be taken into account.

4. Material and Methods

The foundation of the present thesis is 11 sediment cores from the western Svalbard slope (Figure 1). In this section a brief summary on material and methods are given, more details are presented in the respective papers.

4.1. Magnetic Susceptibility

Magnetic susceptibility is a relatively fast and non-destructive parameter to measure, and has years ago proven a very good potential for inter-core correlation (e.g. Radhakrishnamurty et al., 1968; Andrews et al., 1995; Robinson et al., 1995; Kissel et al, 1997). The susceptibility is measured by applying a magnetic field to the material and recording the ability of the material to magnetize. All 11 cores were measured on board for magnetic susceptibility using a loop-sensor connected to a GEOTEK Multi Sensor Core Logger. The loop-sensor MS measurements give a smoothed signal compared to the hand-held point-sensor measurements and mass specific measurements, since the loop sensor measures a signal of not only the part of the core passing through the sensor, but also some cm's on both sides of the level measured.. Seven cores were also measured with a hand-held F-probe type MS2 point-sensor from Bartington Instruments, generally every 2 cm. In two cores, mass specific MS was measured in a discrete sample solenoid-type MS2 sensor on 8 cm^3 samples in plastic boxes every $2 - 2.5$ cm (JM02-463GC, Paper I and JM04-025PC, Paper II) .

4.2. Sampling

Selected cores were sampled in sample frequencies varying from 1 cm to 5 cm between samples in one cm thick slices. Samples were weighed for wet weight, dried and weighed for dry weight. Samples were separated into different grain-size fractions by wet sieving and subsequent dry sieving. Further details and specific sample frequencies are given in the papers.

4.3. Stable Isotopes, δ^{18}O and δ^{13}C

Stable isotopes were measured on the polar planktic foraminifera *Neogloboquadrina pachyderma* s Planktic oxygen isotopes are included in all four papers. Planktic δ^{13}C is includen in papers I, II and IV. Benthic δ^{18}O and δ^{13}C are included in Papers III (Rasmussen, unpublished data).

4.4. Sortable silt

The grain-size of sortable silt (SS) was measured in one core to reconstruct changes in bottom current velocity. Two different methods were used. For the part older than 24 ka, the grain-size was measured on a Sedigraph 5100 using standard procedures (Robinson and McCave, 1994). The part 35–0 ka was measured using a Beckman-Coulter Lazer Diffraction Particle Size Analyzer. The overlap of c. 1 m (covering c. 9 ka) of the core was measured with both methods, and for this overlap the two methods show comparable results (Paper II, Figure 5). The two records are compared and stacked into one record in (Paper II, Figure 5b). Following the argumentation by Hass (2002) neither calcium carbonate nor opal was removed prior to the analyses due to generally very low amounts.

4.5. Ice Rafted Detritus (IRD)

IRD can be studied in many different grain-size fractions and basically all fractions have been used in the literature (see section 3 above). This thesis is no exception. In Paper II, IRD is defined as the weight the residue >63 µm. In Paper I, III and IV IRD was counted on a picking tray under a binocular microscope. At least 300 grains were counted. In samples with less than c. 500 grains all grains were counted. In Paper I, IRD was counted in cores JM03-373PC2 and JM04-025PC in the size fraction >500 µm. In Paper IV, IRD was counted in the size fraction >150 µm in core JM03-373PC2 and >1 mm for the core JM02-460GC/PC. In Paper III, the residue >100 µm was dry sieved into grain-size fractions of 150–250 µm, 250–500 µm, and >500 µm. The fractions 250–500 µm and >500 µm were subsequently counted on a picking tray. Thereafter, the 100–500 µm residue was dry sieved over a 150 µm mesh size and the IRD was also counted in the fraction 150–500 µm. Mineral classes were determined in the size fraction 250–500 µm. Twelve different mineral classes were quantified

in the core JM04-025PC, but only the two dominant mineral classes, fragments of mono-crystalline quartz and siltstones are used.

IRD concentrations (no/g) are calculated relative to the dry weight of the total sample (Papers I, III and IV). The IRD flux in no. grains/cm^2/ka is calculated as follows (Paper III) IRD counts (no. grains/g $_{\text{wet weight}}$) * wet bulk density (g/cm^3) * sedimentation rate (cm/ka).

5. Abstracts

5.1. Paper I: A new Late Weichselian and Holocene marine chronology for the western Svalbard slope 30,000–0 cal years BP

Data have been compiled from eleven sediment cores from 76° to 80°N on the western Svalbard slope. The cores are from water depths between 630 and 1880 m and show clear similarities in lithology and magnetic susceptibility. All cores penetrated into mass transported sediments from glacigenic debris flow events and turbidity flow events. The mass transport probably occurred when the ice reached the shelf edge. The deposits date between 24,080 ±150 and 23,550 ±185 calibrated (cal) years BP. The records also include laminated, fine grained sediments interpreted as deposits from sediment-laden meltwater plumes dated between 14,780 ±220 and 14,300 ±260 cal years BP. In Holocene sediments a diatom rich fine grained layer dates 10,100 ±150 to 9840 ±200 cal years BP. The eleven cores have been stacked into one record with absolute age control from 35 AMS^{14}C dates. Together with oxygen isotope stratigraphy and contents of ice rafted detritus the stacked record provides a useful chronology tool for cores on the western Svalbard slope. Our study improves the age control of earlier well documented glacial events and shows that the maximum glacial state and the onset of the deglaciation both occurred 2500-3000 years earlier than previously reconstructed for the western Svalbard margin. The results indicate that during the last 30,000 years advance and retreat of the Svalbard-Barents Sea Ice Sheet was closely linked to the flow of Atlantic water and Polar water over the margin.

5.2. Paper II: Sortable Silt Cycles in Svalbard Slope Sediments 74-0 ka

Grain-size of sortable silt (SS, 10–63 µm) was studied in sediment core JM04-025PC from the western Svalbard slope to reconstruct the bottom current activity and intermediate water circulation in the Greenland Sea. The SS record covers the last 74 ka and shows consistent millennial scale oscillations in grain size. The youngest part of the record (<25 ka) is well correlated with the few available previously published reconstructions of grain-size from the North Atlantic Ocean and the Nordic seas. Fining of SS occurs during four well known regional cold climatic intervals, the 8.2 ka cold spell, the Younger Dryas and North Atlantic Heinrich Events H1 and H2, as well as during a local melt water event 14.7–14.4 ka, possibly coinciding with the Older Dryas. Also before 25 ka, the grain-size oscillated in pace with the Northern Hemisphere climate with finer grain-sizes during cold periods and coarser grain-sizes during warm periods. The fining of SS indicate reduced bottom current strength and reduced water exchange between the Greenland Sea and the Arctic Ocean during regional climate cooling events, and probably also reduced deep ocean convection in the Greenland Sea gyre.

5.3. Paper III: Ice rafting patterns on the western Svalbard slope 74–0 ka: Interplay between ice sheet activity and ocean circulation

The concentration, composition and grain-size of Ice Rafted Detritus (IRD) are studied in three cores from the western Svalbard slope (1130–1880 m water depth, 76–78°N). The cores cover the period 74–0 ka. The aim is to provide new insight to the dynamics of the Svalbard-Barents Sea Ice Sheet during Marine Isotope Stages (MIS) 4–1 on orbital (glacial/interglacial) and millennial (Dansgaard-Oeschger events of stadial-interstadial) time scales. The concentration, composition and grain-size of IRD vary on both orbital and millennial time scales. The IRD consist mainly of fragments of siltstones and fragments of mono-crystalline transparent quartz (referred to as "quartz"). IRD dominated by siltstones have a local Svalbard-Barents Sea source, while IRD dominated by quartz are from distant sources far from Svalbard. Local siltstone-rich IRD predominates in warmer climatic phases (interstadials), while the relative abundance of allochthonous quartz-rich IRD increases in cold phases (glacials and stadials). During the last glacial maximum 24–16.1 ka, the quartz content reached up to >90%. In warm climate, local iceberg calving apparently increased and the warmer conditions probably caused faster ice melting. During the glacial maxima (MIS 4

and MIS 2) and during cold stadials and Heinrich events, IRD was mostly allochtonous indicative of relatively stable local ice sheets with low ablation. During ice retreat phases of the MIS 4/3- and MIS 2/1 transitions, maxima in IRD deposition dominated by local coarse-grained IRD occur in pulses. These maxima correlate with episodes of climate warming, indicating a rapid, stepwise retreat of the ice.

5.4. Paper IV: Paleoceanographic evolution of the SW Svalbard margin (76°N) since 20,000 ^{14}C yr BP

Two cores from the southwestern shelf and slope of Storfjorden, Svalbard, taken at 389 m and 1485 m water depth have been analyzed for benthic and planktic foraminifera, oxygen isotopes, and ice-rafted debris. The results show that over the last 20,000 yr, Atlantic water has been continuously present on the southwestern Svalbard shelf. However, from 15,000 to 10,000 ^{14}C yr BP, comprising the Heinrich event H1 interval, the Bølling–Allerød interstades and the Younger Dryas stade, it flowed as a subsurface water mass below a layer of polar surface water. In the benthic environment, the shift to interglacial conditions occurred at 10,000 ^{14}C yr BP. Due to the presence of a thin upper layer of polar water, surface conditions remained cold until ca. 9000 ^{14}C yr BP, when the warm Atlantic water finally appeared at the surface. Neither extensive sea ice cover nor large inputs of melt water stopped the inflow of Atlantic water. Its' warm core was merely submerged below the cold polar surface water.

6. Synthesis of papers

6.1. Paper I

6.1.1. Improving the local marine chronology for the western Svalbard slope

The primary focus of Paper I is on magnetic susceptibility and lithology data to establish an absolute chronology of events during the last 30,000 years for the western Svalbard slope. The secondary focus is to relate the new chronology to the glacial history of the Svalbard-Barents Sea Ice Sheet. The paper gives absolute age control for marine sediments from c. 500 to c. 2000 m water depth from numerous AMS-^{14}C dates and wiggle-

matching of records of magnetic susceptibility (Figures 3–4 in Paper I). The synchronization is further tied to three distinct lithological units found in all cores along the slope.

The magnetic susceptibility pattern displays two very distinct intervals with low susceptibility. The upper interval consists of a fine-grained laminated layer. This interval is interpreted as a melt water deposit, and dated to 14.7–14.4 ka. The lower interval is dark colored and in most cores very coarse grained and interpreted as glacigenic mass transport deposits. This unit is dated to 24.1–23.5 ka. These two low-susceptibility-intervals provide four tie-points for the chronology. Two more tie-points are provided from the lithology as the cores with Holocene sediments include a layer with high abundance of diatoms (*Coscinodiscus* spp). The diatom layer is dated to 10.1–9.8 ka and consists of fine grained sediments deposited by high sedimentation rate. The diatom layer is interpreted as the result of the passing of the northward migrating Polar Front. Three other distinct patterns in magnetic susceptibility are further used as tie-points in the chronology. A total of nine tie-points are given absolute ages with an estimated uncertainty of c. twice the uncertainty of the AMS^{14}C method (Figure 5).

If magnetic susceptibility is measured on board during a cruise, the comparison with stacked record may give an initial age model within hours of retrieval. For the last decade our research group has exploited this on several cruises to the western Svalbard slope. Paper I gives other scientists the same opportunity (e.g., Pedrosa et al., 2011; Sztybor et al., 2012; Lucchi et al., 2013, Consolaro et al., 2014).

Paper III presents two up-dates of the chronology. The first one is a very important update to the chronology regarding the low susceptibility unit interpreted as glacigenic mass transported sediments. The mass transport probably occurred when the ice reached the shelf edge (e.g., Laberg and Vorren, 1995; Dimakis et al., 2000). Linear interpolation of the nearest two AMS^{14}C dated levels above the mass transport deposits in four different regions all gave between c. 24.1–23.5 ±0.2 ka, which is a range too narrow to discriminate between the ages of the deposits (Figure 3 in Paper I). In Paper I, we state that stratigraphically, the deposits can be regarded as synchronous within the uncertainties of the AMS^{14}C dating method. In Paper III, this statement is strengthened. The top of the interval with low susceptibility (i.e., Tie-point 7, Figure 5) is interpreted as a true stratigraphic marker. In Paper III, the top of the low susceptibility interval is interpreted as a wide-spread deposit of ice rafted detritus blanketing all 11 core sites on the slope. The IRD is interpreted to come from a collapsing ice stream or ice shelf in the Storfjorden trough (see section 6.3 below). Also Paper III adds one more tie-point to the chronology, labeled Tie-Point 6.1 (Paper III, Figures 2,4). Tie-point 6.1 is defined

as a combination of a steep decline in magnetic susceptibility, a local maximum in IRD-concentration and coarsening of IRD. The calibrated age of Tie-point 6.1 is 20.17 ka estimated from the age model of the core JM03-373PC (Paper III, Figure 4, Table 1).

6.1.2. Glacial history of the Svalbard-Barents Sea Ice Sheet

The history of Svalbard Barents Sea Ice Sheet has been studied in great detail (Ingólfsson and Landvik, 2013) both from terrestrial (e.g., Svendsen and Mangerud, 1997; Mangerud et al., 1998) and marine records (e.g. Elverhøy, et al., 1995; Andersen et al., 1996; Dokken and Hald, 1996; Landvik et al., 1998; Mangerud et al., 1998) as well as by numerical modeling (e.g., Siegert and Dowdeswell, 1995a,b, 2002, 2004). The main contribution of Paper I is an improvement of the marine chronology by high resolution and well-dated core material.

6.1.2.1. Age estimation of mass transport deposits and thereby the peak glaciation

For the previous reconstruction presented by the PONAM project (Elverhøi et al., 1995; Landvik et al., 1998), only one mass transport deposit on the western Svalbard slope was well dated, a turbidite in core NP90-21 from 2130 m water depth on the Isfjorden Trough Mouth Fan (given a minimum age of c. 23.2 ka). We managed to provide mass transport deposits from four different regions of the slope with absolute age estimates ranging from 23.5 to 24.1 ka (section 6.1.1). The ages were estimated by linear interpolation of the two nearest AMS^{14}C dates above the deposits following Owen et al. (2007). In three of the regions we also dated sediments below the mass transport deposits to obtain maximum ages of the deposition (ranging from 24.05 ±0.18 to 26.93 ±0.25 ka, Paper I, Figure 3, Table 2).

Mass transport deposits are regarded as monitors of a fully glaciated shelf, and hence the maximum extent of the ice sheet (Laberg and Vorren, 1995; Vorren and Laberg, 1997; King et al., 1998; Dimakis et al., 2000; Dowdeswell and Elverhøi, 2002). The absolute ages of c. 24 ka was c. 3 ka older than earlier suggested ages for the maximum glaciation of western Svalbard (Elverhøi, et al., 1995; Mangerud et al., 1998). The implication is that it appears that the entire western margin of Svalbard was fully glaciated c. 3 ka earlier than suggested by previous reconstructions.

Also the initial retreat from the shelf occurred several ka earlier than the previously suggested timing of c. 18 ka (Elverhøi, et al., 1995; Mangerud et al., 1998). The main evidence for glacial retreat prior to 20 ka is the appearance of hemipelagic sediments on former glaciated outer shelf areas with ages around 20 ka (e.g., Cadman, 1996; Ślubowska-

Woldengen et al., 2007) (Paper IV). The IRD record in Paper III points to that the main part of early ice retreat occur already around 24 ka (section 6.3.1.).

6.1.2.2. A melt water plume at c. 14.5 ka

A thick package of fine-grained laminated sediments is documented all along the western Svalbard slope (Paper I, Figures, 3–6). The age model estimates an age within the Bølling interstadial. The deposit is thinning towards the north and towards greater water depths from the upper part of the slope of the Storfjorden trough-mouth Fan, and with a thicker unit on the upper slope than in a core from the shelf (Paper IV), which is inconsistent with a local Storfjorden source. In Paper I, we suggest that the melt water came from a southern source, probably the southern Barents Sea. Recently, Lucchi et al. (2013) has added the southern part of the Storfjorden Trough-mouth fan and the Kvithola fan to the areas with fine-grained laminated sediments of the same age, and their sediment distribution confirms a source south of Storfjorden. They suggest the Kvithola ice dome as a possible source for the melt water. Fine-grained units of c. the same age are also found in the southern Barents Sea (Aagaard-Sørensen et al, 2010; Junttila et al., 2010) and the northern Barents Sea (Lubinski et al., 1996). The age of the melt water discharge has been refined by Lucchi et al. (2013) to c. 14.5 ka and they suggest that this event correlates with the Older Dryas cold interval and provided a significant contribution to the so-called Melt Water Pulse 1a of the last deglaciation (e.g., Fairbanks, 1989; Stanford et al., 2006).

6.1.2.3. A diatom layer marking the passing of the northward migrating Polar Front

The new chronology contributes to the paleoceanography of the early Holocene by timing the northward passing of the Polar Front west of Svalbard to 10.1–9.8 ka. Establishing the timing of the front passage at Svalbard allows an estimation of the speed of the northward migration. In the southern part of the Nordic Seas at c. 60 °N the front passing occurred c. 1600 years earlier (Stabell, 1986; Koç-Karpuz and Jansen, 1992; Nees et al., 1997). A northward migration of c. 16° in 1600 years gives an average front movement of c. 1° pr century. The corresponding average speed of c. 1 km pr year shall only be regarded as a crudely smoothed average. The migration was probably step-wise (Ebbesen et al., 2007; Hald et al., 2007).

6.2. Paper II reconstruction of bottom current strength

Paper II aims to reconstruct bottom currents on centennial time scale by studying changes in grain-size in a long piston core record from the western Svalbard margin covering the last 74 ka (Paper II, Figures 5,7). Previous grain-size based bottom current reconstructions from the western Svalbard slope and the Fram Strait has only been published from two cores, one covering the last 17 ka (Hass, 2002; Birgel and Hass, 2004) and one core covering the last 9 ka (Werner et al., 2013). Grain-size of sortable silt is regarded the most reliable 'paleo-current meter' (McCave et al., 1995; McCave and Hall, 2006). The record presented in Paper II is the first in the Nordic Seas to include the entire Marine Isotope Stages MIS 4– MIS 2. The grain-size of sortable silt seems to fit with a near peak-to-peak correlation with magnetic susceptibility measurements in the southern Norwegian Sea (Paper II, Figure 7). This magnetic susceptibility signal is positively correlated with interstadial/stadial climate shifts (e.g., Rasmussen et al., 1996a) and with a 5 ka long grain-size record from the southern Norwegian Sea at 61°N (Ballini et al., 2006). The magnetic susceptibility signal is generally believed to display changes in magnetic grain-size and proposed reflect bottom current strength (e.g., Rasmussen et al., 1996a, 1998; Kissel et al., 1997, Moros et al., 1997, 2004). Thus it seems that the bottom current dynamics on the western Svalbard slope varies in pace with the southern Norwegian Sea and North Atlantic and the strength of outflow of deep- and intermediate water over the Greenland-Scotland Ridge. In the paper, we argue that the grain-size on the western Svalbard slope may reflect changes in the strength of open ocean convection in the Greenland Sea. However, the reconstruction presented in Paper II is based on only one core (similar to e.g., Hass, 2002; Birgel and Hass, 2004; Praetorius et al., 2008; Werner et al., 2013), and as suggested in section 7.2 more records could - and should - be included in the future. One important issue when using just one core is that the water masses can migrate up-/down slope together with changes in the current strength (e.g., Thornalley et al., 2013) or be detached from the slope (Kuijpers et al., 2002). Another possible issue is that local down-slope currents can sort sortable silt equally well – or better – than regional along slope currents. Both issues are potential pit-falls when analysing just one core record (e.g., McCave and Hall, 2006).

The core JM04-025PC seems not to be strongly affected by down-slope currents. For instance, no clear cross-beddings are visible on X-rays. We have cores from the slope where cross beddings are visible. These cores are from the rim of canals and are not part of this thesis (but one of them has been studied in the course GEO3111 in 2007 with the thesis author

as course responsible). Also it seems unlikely that the 11 cores from four different regions of the slope should display similar magnetic susceptibility patterns if any of the cores were affected by local down-slope currents (Paper I, and section 6.1). According to the similar magnetic susceptibility and lithology of all the studied cores, they display regional slope-wide signals more than local signals. The possibility of up- or down-slope current migration cannot be solved from studies of just one core. However, even if the sortable slit record presented in Paper II turns out to be strongly affected by up- or down slope current migration, the record should still reflect changes in the regional bottom current dynamics on millennial scale.

6.3. Paper III: Ice sheet activity deduced from Ice Rafted Detritus (IRD)

Paper III targets ice rafted detritus (IRD) with the main aim to reconstruct the activity of the local Svalbard-Barents Sea Ice Sheet on orbital and millennial time scale. Potentials and problems related to reconstructing ice sheet activity from IRD are presented in section 3. We use end-member modeling to extract the variability in local and coarse grained IRD and thereby the ice rafting from local icebergs. Local siltstone-rich, iceberg rafted IRD mainly appears in warm, interstadials climate (Paper III, Figure 10). In cold, stadial climate the IRD is to a higher degree quartz-rich, long transported and fine grained. Possibly with a higher proportion of sea ice rafted IRD. We suggest the millennial scale IRD pattern to reflect a combination of 1. A more active local ice sheet in warmer climate, and 2. The fact that ice melt closer to its source in warmer waters.

6.3.1. Ice sheet growth and decay – Timing and causation

The growth and decay of the Svalbard-Barents Sea Ice Sheet has previously been linked to the moisture supply from the ocean, i.e., changes in accumulation of snow (Hebbeln et al., 1994). However, the growth and decay of ice sheets depends on the balance between accumulation and ablation. In Paper I the initial retreat is suggested to occur at 21–20 ka, In Paper III we suggest that the retreat starts already at 24 ka. 24–20 ka was a period with very low solar insolation (Laskar et al., 2004) where we would expect the ice to advance and not retreat (Paper I, Figure 6). However, other factors than high solar insolation can lead to increased ablation. A thickening ice sheet can get too thick to be stable. When a certain thickness is reached, the combination of higher isolation and increased pressure from the ice can lead to a switch from a cold based ice sheet to a warm based ice sheet. This switch can trigger sliding, surging and massive ice loss (MacAyeal, 1993a). Increased oceanic heat

transport can result in rapid ice shelf disintegration and a following activation of ice streams (Hulbe, 1997; Hulbe et al., 2004; Shaffer et al., 2004; Marcott et al., 2011). Also a rising sea level, for instance after a Heinrich Event, can de-stabilize an ice sheet and lead to a retreat of the grounding line (Benn et al., 2007). At c. 23.5 ka, a widespread IRD layer was deposited along the western Svalbard slope (Paper III, Figures 2–5). In the cores of the present thesis, this IRD layer overlies mass transported sediments (Section 6.1). Recent studies has shown the IRD layer is also present in records without mass transport deposits (Sztybor et al., 2012; Zamelzcyk et al., 2013; Chauhan et al., 2014). It is likely IRD from this ice rafting event that was found in sediments from the central Norwegian Sea by Bauch et al. (2001) (Paper I). The widespread deposition of IRD at the time, we interpret as a result of increased ice stream activity leading to a massive discharge of icebergs. Massive iceberg discharge means intensified ablation. The timing correlates well with the timing of land based thinning of the ice sheet (Gjermundsen et al., 2013; Hormes et al., 2013) and the presence of mega-scale glacial lineations in Storfjorden Trough (Ottesen et al., 2005, 2007; Andreassen et al., 2008). The timing is within the time frame of Heinrich Event 2 and Greenland Interstadial 2 (Zamelczyk et al., 2014; Rasmussen et al., 2014).

The build-up phase for the ice sheet is characterized by absence of local IRD on the western Svalbard slope. This, combined with low sedimentation rates on the slope (Paper I) points to growth of a very stable local ice sheet, not losing a significant amount of its mass. As suggested in Paper I, this points toward a cold based ice sheet. Low IRD concentrations and very low sedimentation rates during the glacial growth phase is also documented in a core north of Svalbard (Knies et al., 1999). A glacial growth phase characterized by low ablation followed by a fast high-ablation retreat phase is similar to the 'binge/purge model' of MacAyeal (1993a,b).

6.4. Paper IV Paleoceanography 24–0 ka

6.4.1. Paleo-temperature profiles over the Storfjorden Trough-mouth Fan

A main result of Paper IV is qualitative paleo-temperature profiles for the last 20,000 ^{14}C years, i.e. 24–0 calibrated ka (calibrated ages are derived from Paper I). The result is based on a thorough fauna study of planktic and benthic foraminifera from two cores, JM02-460GC/PC from 389 m and JM03-373PC from 1485 m water depth. Also stable isotopes from planktic and benthic foraminifera is measured and IRD was counted. The fauna study documents a continuous presence of warm Atlantic water since 24 ka. The Atlantic water was

submerged under a layer of fresh water from H1 (c. 17 ka) until 10.1 ka in the early Holocene. During the very cold climate interval of North Atlantic Heinrich Event 1 (H1) c. 17-15.5 ka and Younger Dryas (YD), 12.7-11.7 ka, the melt water appears to be adverted from foreign sources (Paper I and III). During the Bølling-Allerød Interstadials (c. 15.5–12.7 ka) and early part of the Holocene 11.7–10.1 ka, the blanketing melt water came from the disintegrating Svalbard-Barents Sea Ice Sheet. During the Bølling-Allerød interstadial, the water temperature at 300–400 m was higher than during the Holocene (Ślubowska-Woldengen et al., 2007).

6.4.2. IRD and isotopes reflecting sea ice changes

The IRD counts in core JM03-373PC on mainly fine grained sand (>150 μm, Paper IV, Figure 5n) show high IRD concentrations around 16 and 18 ^{14}C kyr (c. 19 and 22 ka). These IRD maxima are not visible in the coarse sand fraction (>500 μm, Papers I and III). Probably the IRD to a high degree is delivered by sea ice from the Arctic Ocean (Paper III). Also the Holocene IRD increase since c. 6 ka is mainly seen in the fine-grained IRD fraction, and most likely a result of increasing sea ice cover (Papers I and III) (Werner et al., 2013). A comparison of benthic oxygen isotopes from JM02-460GC/PC in Storfjorden Trough and a core from Hinlopen Trough on the northern Svalbard shelf show very similar values during the early Holocene until c. 8.9 calibrated ka (8 ^{14}C kyr). After 8.9 ka the oxygen isotope values in are higher in Storfjorden Trough than on the northern Svalbard shelf. The difference increases at c. 5.8 ka (5 ^{14}C kyr). The isotope difference is proposed to be the result of increased sea ice production and thereby increased brine formation in Storfjorden. The benthic fauna in cores from Storfjorden and the Storfjorden Trough similarly points to a two-step Holocene cooling, with an initial increase in brine formation from c. 8.2 ka and further cooling at c. 5 ka (Rasmussen and Thomsen, 2015).

7. Future work

7.1. An updated glaciation curve for MIS4–1

The stacked magnetic susceptibility record and the age estimation of mass transport deposits points to a relatively uniform behavior of the ice sheet over the entire western slope.

However, as pointed out by Ingólfsson and Landvik (2013) the outcome of a study of the Svalbard-Barents Sea Ice Sheet depends on the methods used and the "point of view". Terrestrial studies (e.g. Alexanderson et al., 2011; Landvik et al., 2013, 2014) and seismic studies from the Barents Sea (e.g., Ottesen et al., 2005, 2007; Andreassen et al., 2008; Rüther et al., 2011) points to different behavior of different parts of the ice sheet. The recent review by Hormes et al (2013) is a good example of the strength in combining results from studies within the previously glaciated area and cores from the adjacent slope. However, the reviews by Hormes et al. (2013) and Paper I in the present thesis only reach back to 30 ka. The apparent discrepancy between the slope records and records from within the previously glaciated area is one question to resolve for future research (Ingólfsson and Landvik, 2013).

Paper III suggests an update of the glaciation history for the northwestern part of the Svalbard Barents Sea ice sheet 74–0 ka. The resulting glaciation curve would mainly reflect two predominant cycles, the 41 ka obliquity cycle and the 1–2 ka interstadial/stadial cycle. To fill in further details would require a thorough review of the data presented within the last five years as well as a re-assessment of the data and literature reviewed in Paper I. Also other methods for tracing IRD and melt water provenance can be included. Several trace elements has been used to determine the provenance of glacigenic deposits from ice rafting and melt water transportation around the polar North Atlantic (e.g., Grousset et al., 2000; Moros et al., 2002, 2004; Jullien et al., 2006; Crocket et al., 2012, 2013). The study of clay minerology (e.g., Vogt and Knies, 2008, 2009; Junttila et al., 2010; Lucchi et al., 2013) and a novel method for tracing quartz grains to their source (Müller and Knies, 2013) has been tested for the Barents Sea and Svalbard, respectively. The counts of IRD might be done faster and more detailed by using digital image analysis. By training software to recognize IRD, different mineral grains and the roundedness of grains can be determined. The use of digital image analysis may allow more records to be studied during the same amount of time. Also an image analysis tool can be more objective than a person looking into a microscope. The roundedness of grains is omitted from this thesis mainly because the estimation would be subjective and to a high degree dependent on the eyes of the IRD-counter – in addition to being very time consuming. A software tool under development has been tested for measuring circumference and changes in angles to achieve an objective estimate of roundedness (R. Heilbronner, pers comm.). This may improve the separation between iceberg- and sea ice rafted grains. Also the possibility of using filters and contrast stretching might ease mineral determination. Similar to the use of image analysis in GIS (Geographical Information Systems) the software can be trained to do most of the analysis leaving the scientists to do mainly quality control.

No matter which IRD provenance methods chosen, the mass transport deposits on the western Svalbard slope, and till deposits from the shelf and fjords can serve as 'ground truth' for local IRD. By using digital image analysis it should be possible to train the software with IRD from samples from all over the North Atlantic, Nordic Seas and Arctic Ocean, thereby improving significantly the provenance studies by better determining possible end-members for IRD composition and better distinguish between different source areas. If a sufficient amount of well dated and inter-correlated core material is used, it should be possible to use GIS to create maps with contour plots showing the distribution of sand from various sources for icebergs and sea ice at specified time intervals to obtain information about calving from different ice masses, surface current patterns and ice melting.

7.2. Towards a 4D-reconstruction of the bottom current and estimation of heat fluxes for the western Svalbard margin.

The thesis may be used as a stepping stone towards a reconstruction of the bottom current dynamics on the western Svalbard slope in 4D. The cores presented in Paper I measured for sortable silt (Paper II) could provide a series of 3D reconstructions of the bottom current strength at various water depths within time slices of c. 200 years. All cores presented in Paper I and several cores retrieved since 2006 could be included (e.g., Sztybor, 2012; Lucchi et al., 2013; Zamelzcyk et al., 2013; Chauhan et al., 2014). The chronology presented in Paper I provides a foundation for a detailed study of the last 30 ka in centennial resolution. A 4D model of the current strength may allow quantitative estimations of the volume of water moving along the slope. Water volume transportation multiplied with the temperature gradient will be a quantification of the heat-flux from the ocean along the western Svalbard slope. Temperature gradients can be estimated from quantitative temperature proxies either from fauna studies and transfer functions and/or measurements of magnesium/calcium on planktic foraminifera and benthic foraminifera. By including material from other regions in the Nordic seas a basin wide estimate of water and heat flux could be achieved. Paper II correlates the western Svalbard slope to the southern Norwegian Sea, and the southern Norwegian Sea is already correlated to the North Atlantic based on magnetic susceptibility (e.g., Kissel et al., 1999; Eliott et al., 2001).

8. References

Aagaard, K., C. Darnall, and P. Greisman (1973), Year-long current measurements in the Greenland-Spitsbergen passage, *Deep-Sea Res.* 20, 743–746.

Aagaard K, J. H. Swift, and E. C. Carmack (1985), Thermohaline Circulation in the Arctic Mediterranean Seas, *J. Geophys. Res.* 90(C3), 4833–4846.

Aagaard-Sørensen, S., K. Husum, M. Hald, and J. Knies (2010), Paleoceanographic development in the SW Barents Sea during the Late Weichselian-Early Holocene transition. *Quaternary Sci. Rev.* 29 (25-26), 3442–3456.

Alexanderson H., J. Y. Landvik, and J. Y. Ryen (2011), Chronology and styles of glaciation in an inter-fjord setting, northwestern Svalbard, *Boreas* 39(2), 367–376.

Alexanderson, H., J. Backman, T. M. Cronin, S. Funder, Ó. Ingólfsson, M. Jakobsson, J. Y. Landvik, L. Löwemark, J. Mangerud, C. März, P. Möller, M. O'Regan, and R. F. Spielhagen (2014), An Arctic perspective on dating Mid-Late Pleistocene environmental history, *Quaternary Sci. Rew.* 92, 9–31.

Alley, R. B., and D. R. MacAyeal (1994), Ice-rafted debris associated with binge/purge oscillations of the Laurentide Ice Sheet, *Paleoceanography*, 9(4), 503–511.

Andersen, E. S., T. M. Dokken , A. Elverhøi, A. Solheim, and I. Fossen (1996), Late Quaternary sedimentation and glacial history of the Western Svalbard continental margin, *Mar. Geol.* 133, 123–156.

Andreassen, K., J. S. Laberg, and T. O. Vorren (2008), Seafloor geomorphology of the SW Barents Sea and its glaci-dynamic implications, *Geomorphol.* 97, 157–177.

Andrews, J. (2000), Icebergs and iceberg rafted detritus in the North Atlantic: facts and assumptions, *Oceanography* 13(3), 100–108.

Andrews, J. T., B. Maclean, M. Kerwin, W. Manley, A. E. Jennings, and F. Hall (1995), Final stages in the collapse of the Laurentide Ice Sheet, Hudson Strait, Canada, NWT: 14C AMS dates, seismic stratigraphy, and magnetic susceptibility logs, *Quaternary Sci. Rev.* 14 (10), 983–1004.

Bauch, H. A., H. Erlendkeuser, R. F. Spielhagen, U. Struck, J. Matthiessen, J. Thiede, and J. Heinemeier (2001), A multiproxy reconstruction of the evolution of deep and surface waters in the subarctic Nordic seas over the last 30,000 yr, *Quaternary Sci. Rev.* 20, 659–678.

Bauch, H. A., E. S. Kandiano, and J. P. Helmke (2012), Contrasting ocean changes between the subpolar and polar North Atlantic during the past 135 ka, *Geophys. Res. Lett.* 39(11), L11604, doi:10.1029/2012GL051800.

Benn, D., C. R. Warren, and R. H. Mottram (2007), Calving processes and the dynamics of calving glaciers, Earth-Sci. Rev. 82, 143–179.

Bischof, J. F. (2000), Ice Drift, Ocean Circulation and Climate Change, Springer-Praxis,Cornwall. 215pp.

Bischof, J. F., and D.A. Darby (1997), Mid- to late Pleisticene Ice Drift in the western Arctic Ocean: Evidence for a different Circulation in the past, *Science 277,* 74–77.

Bond, G., and R. Lotti (1995), Iceberg discharge into the North Atlantic on millennial timescales during the last glaciations, *Science* 267, 1005–1010.

Bond, G., H. Heinrich, W. Broecker, L. Labeyrie, J. McManus, J. Andrews, S. Huon, R. Jantschik, S. Clasen, C. Simet, K. Tedesco, M. Klas, G. Bonati, and S. Ivy (1992), Evidence for massive discharges of icebergs into the North Atlantic ocean during the last glacial period, *Nature* 360, 245–249.

Bond, G., W. Broecker, S. Johnsen, J. McManus, L. Labeyrie, J. Jouzel, and G. Bonani (1993), Correlations between climate records from North Atlantic and Greenland ice, *Nature,* 365, 343–347.

Bond, G. C., W. Showers, M. Cheseby, R. Lotti, P. Almasi, P. deMenocal, P. Priore, H. Cullen, I. Hajdas, and G. Bonani (1997), A pervasive millennial-scale cycle in North Atlantic Holocene and Glacial climates, *Science* 278, 1257–1266.

Bond, G. C., W. Showers, M. Elliot, M. Evans, R. Lotti, I. Hajdas, G. Bonani, and S. Johnsen (1999), The North Atlantic's 1-2 kyr Climate Rhythm: Relation to Heinrich Events, Dansgaard/Oeschger Cycles and the Little Ice Age. *In* Clark, P. U., R. S. Webb and L. D. Keigwin (eds.), Mechanisms of Global Climate Change at Millennial Time Scales, *Geophys. Monogr. 112*, AGU, 35–58.

Bondevik, S., J. Mangerud, H. H. Birks, S. Gulliksen, and P. Reimer (2006), Changes in North Atlantic radiocarbon reservoir age during the Allerød and Younger Dryas, *Science* 312, 1514–1517.

Birgel, D., and H. C. Hass (2004), Oceanic and atmospheric variations during the last deglaciation in the Fram Strait (Arctic Ocean): a coupled high-resolution organic-geochemical and sedimentological study. *Quaternary Sci. Rev.* 23, 29-47.

Cadman, V. (1996), Glacimarine sedimentation and environmants during the late Weichselian and Holocene in the Bellsund Through and van Keulenfjorden, Svalbard, Unpublished Ph. D. thesis, University of Cambridge.

Chauhan, T., T. L. Rasmussen, R. Noormets, M. Jacobsson, and K. A. Hogan (2014), Glacial history and paleoceanography of the southern Yermak Plateau since 132 ka BP, *Quaternary Sci. Rev.* 92, 155–169, doi: 10.1016/j.quascirev.2013.10.023

Consolaro, C., T. L. Rasmussen, G. Panieri, J. Mienert, S. Bünz, and K. Sztybor (2014), Carbon isotopes (δ^{13}C) excursions suggest times of major methane release during the last 14 ka in Fram Strait, the deep-water gateway to the Arctic, Clim. Past. Discuss. 10, 4191–4227. doi:10.5194/cpd-10-4191-2014.

Crocket, K. C., D. Vance, G. L. Foster, D. A. Richards, and M. Tranter (2012), Continental weathering fluxes during the last Glacial/Interglacial cycle: insight from the marine sedimentary Pb record at Orphan Knoll, NW Atlantic, *Quaternary Sci. Rev.* 38, 89–99.

Crocket, K., G. L. Foster, D. Vance, D. A. Richards, and M. Tranter (2013), A Pb isotopic tracer of ocean-ice sheet interaction: the record from the NE Atlantic during the Last Glacial/Interglacial cycle, *Quaternary Sci. Rev.* 82, 133–144.

d'Errico, F., and M. F. Sánchez Goñi (2003), Neandertal extinction and the millennial scale climatic variability of OIS 3, *Quaternary, Sci. Rev.* 22(8), 769–788.

Darby, D. A., and P. Zimmerman (2008), Ice-rafted detritus events in the Arctic during the last glacial interval, and the timing of the Innuitian and Laurentide ice sheet calving events, *Pol. Res. 27, 114*–127,

Dimakis, P., A. Elverhøi, K. Høeg, A. Solheim, C. Harbitz, J. S. Laberg, T. O. Vorren, and J. Marr (2000). Submarine slope stability on high-latitude glaciated Svalbard–Barents Sea margin, *Mar. Geol.,* 162, 303–316.

Dokken, T., and M. Hald (1996), Rapid climatic shifts during isotope stages 2–4 in the Polar North Atlantic, *Geology* 24, 599–602.

Domack, E., P. O'Brien, P. Harris, F. Taylor, P. G. Quilty, L. De Santis, and B. Raker (1998), Late Quaternary sediment facies in Prydz Bay, East Antarctica and their relationship to glacial advance onto the continental shalf, *Antarc. Sci.* 10(3), 236–246.

Dowdeswell, J. A., and T. Murray (1990), Modelling rates of sedimentation from icebergs, *In* Dowdeswell J. A., and J. D. Scourse (eds.), *Glacimarine Environments: Processes and Sediments*, Geol. Soc, London,. Spec. Publ., 53, 121–137.

Dowdeswell, J.A., and A. Elverhøi, (2002), The timing of initiation of fast-flowing ice streams during a glacial cycle inferred from glacimarine sedimentation, *Mar. Geol.* 188, 3–14.

Ebbesen, H., M. Hald, and T. H. Eplet (2007), Late glacial and early Holocene climatic oscillations on the western Svalbard margin, European Arctic, *Quat Sci. Rev.* 26, 1999–2011.

Eiken, O., and K. Hinz (1993), Contourites in the Fram Strait, *In* Stow, D. A. and J.-C. Faugères (eds.), Contourites and Bottom Currents, *Sediment. Geol.,* 82, 15–32.

Eldevik, T., J. E. Ø. Nilsen, D. Iovino, K. A. Olsson, A. B. Sandø, and H. Drange (2009), Observed sources and variability of Nordic seas overflow, N*ature Geoscience DOI:10.1038/NGEO518*

Eliott, M., L. Labeyrie, T. Dokken, and S. Manthé (2001), Coherent patterns of ice-rafted debris in the Nordic regions during the last glacial (10–60 ka), *Earth and Plan. Sci. Lett.* 194, 151–163.

Elverhøi, A., and A. Solheim (1983), The Barents Sea ice sheet – a sedimentologigal discussion, *Pol. Res.* 1 n.s., 23–42.

Elverhøi, A., E. S. Andersen, T. Dokken, D. Hebbeln, R. Spielhagen, J. I. Svendsen, M. Sørflaten, A. Rørnes, M. Hald, and C. F. Forsberg (1995), The Growthe and Decay of the Late Weichselian Ice Sheet in Western Svalbard and Adjacent Areas Based on Provenance Studies of Marine Sediments, *Quaternary Res. 44,* 303–316.

Elverhøi, A., J. A. Dowdeswell, S. Funder, J. Mangerud, and R. Stein (1998), Glacial and oceanic history of the Polar North Atlantic margins: an overview, *Quaternary Sci. Rev.* 17 (1-3), 1-10.

Elverhøi, A., F. V. de Blasio, F. A. Butt, D. Issler, C. Harbitz, L. Engvik, A Solheim, and J. Marr (2002), Submarine mass-wasting on glacially-influenced continental slopes: processes and dynamics. *In* Dowdeswell, J.A., and C. Ó Cofaigh (eds.), Glacier-Influenced Sedimentation on High-Latitude Continental Margins. Geological Society, *London, Special Publications* 203, 73–83.

Fahrbach, E., J. Meincke, S. Østerhus, G. Rohardt, U. Schauer, V. Tverberg, and J. Verduin (2001), Direct measurements of volume transports through Fram Strait. *Pol. Res.* 20 (2), 217–224.

Faleide, J. I., A. Solheim, A. Fiedler, B. O. Hjelstuen, E. S. Andersen, and K. Vanneste (1996), Late Cenozoic evolution of the western Barents Sea–Svalbard continental margin, *Glob. and Plan. Change* 12, 53–74.

Fairbanks, R. G. (1989), A 17,000-year glacio-eustatic sea level record: Influence of glacial melting rates on the Younger Dryas event and deep-ocean circulation, *Nature* 342, 637–642

Forwick, M., and T. O. Vorren (2009), Late Weichselian and Holocene sedimentary environments and ice rafting in Isfjorden, Spitsbergen, *Palaeogeogr., Palaeoclimatol., Palaeoecol.*, 280 (1-2), 258–274.

Gjermundsen, E. F., J. P. Briner, N. Akcar, O. Salvigsen, P. Kubik, N. Gantert, and A. Hormes (2013), Late Weichselian local ice dome configuration and chronology in Northwestern Svalbard: early thinning, late retreat, *Quaternary Sci. Rev.* 72, 112–127.

Grobe, H. (1987), A simple method for the determination of ice-rafted debris in sediment cores, *Polarforschung* 57, 123–126.

Grotefendt, K., K. Logemann, D. Quadfasel, and S. Ronski (1998), Is the Arctic Ocean warming? *J. Geophys. Res.* 103 (C12), 27,679–27,687.

Grousset, F. E., C. Pujol, L. Labeyrie, G. Auffret, and A. Boelaert (2000), Were the North Atlantic Heinrich events triggered by the behavior of the European ice sheets?, *Geology* 28(2), 123–126.

Haake, F. –W., and U. Pflaumann (1989), Late Pleistocene foraminiferal stratigraphy on the Vöring Plateau Norwegian Sea. *Boreas* 18, 343–356.

Hald, M., T. M. Dokken, and G. Mikaelsen (2001), Abrupt climatic change during the last interglacial–glacial cycle in the polar North Atlantic, *Marine Geology* 176, 121–137.

Hald, M., H. Ebbesen, M. Forwick, F. Godtleibsen, L. Khomenko, S. Korsun, L. R. Olsen, and T. O. Vorren, Holocene paleoceanograhy and glacial history of the West Spitsbergen area, Euro-Arctic margin, *Quaternary Sci. Rev.* 23, 2075–2088.

Hald, M., C. Andersson, H. Ebbesen, E. Jansen, D. Klitgaard-Kristensen, B. Risebrobakken, G. R. Salomonsen, M. Sarnthein, H. P. Sejrup, and R. J. Telford (2007), Variations in temperature and extent of Atlantic Water in the northern North Atlantic during the Holocene, *Quaternary Sci. Rev* 26 (25-28), 3423–3440.

Hass, H. C. (2002), A method to reduce the influence of ice-rafted debris on a grain size record from northern Fram Strait, Arctic Ocean, *Pol. Res.* 21, 299–306.

Hebbeln, D., T. Dokken, E. S. Andersen, M. Hald, and A. Elverhøi (1994), Moisture supply for northern ice sheet growth during the last Glacial Maximum, *Nature* 370, 357–360.

Heinrich, H. (1988), Origin and Consequences of Cyclic Ice Rafting in the Northeast Atlantic Ocean during the Past 130.000 Years, *Quaternary Res.* 29, 142–152.

Hjelstuen, B. O., A. Elverhøi, and J. I. Falaide (1996), Cenozoic erosion and sediment yield in the drainage area of the Storfjorden Fan, *Glob. and Plan. Change* 12, 95–117.

Hormes, A., E. F. Gjermundsen, and T. L. Rasmussen (2013), From mountain top to the deep sea – deglaciation in 4D of the northwestern Barents Sea ice sheet. *Quaternary Sci. Rev.* 75, 78–99.

Hopkins, T. S. (1991), The GIN Sea – A synthesis of its physical oceanography and literature review 1972-1985, *Earth-Sci. Rev., 30,* 175–318.

Houmark-Nielsen, M. (1999), A Lithostratigraphy of Weichselian glacial and interstadials deposits in Denmark, *Bulletins of the Geological Society of Denmark* 46, 101–114.

Howe, J. A., T. M. Shimmield, and R. Harland, (2008), Late Quaternary contourites and glaciomarine sedimentation in the Fram Strait, *Sedimentology* 55, 179–200. doi: 10.111/j.1365-3091.2008.00897.x

Hulbe, C. L. (1997), An ice shelf mechanism for Heinrich layer production, *Paleoceanography* 12(5), 711–717.

Hulbe, C. L., D. R. MacAyeal, G. H. Denton, J. Kleman, and T. V. Lowell (2004), Catastrophic ice shelf
breakup as the source of Heinrich event icebergs, *Paleoceanography*, 19, PA1004,
doi:10.1029/2003PA000890

Ingólfsson, Ó., and J. Y. Landvik (2013), The Svalbard-Barents Sea ice-sheet – Historical, current and future
perspectives, *Quaternary Sci. Rev.* 64, 33–60.

Jessen, S. P. (2005), Dangaard/Oeschger cycler på Svalbardmarginen, Unpublished cand. scient. thesis, Institute
of Geography, University of Copenhagen (in Danish), 73 pp

Jones, G. A., and L. D. Keigvin (1988), Evidence from Fram Strait (78° N) for early deglaciation, *Nature* 336,
56–59.

Jullien, E., F. E. Grousset, S. R. Hemming, V. L. Peck, I. R. Hall, C. Jeantet, and I. Billy (2006), Contrasting
conditions preceding MIS3 and MIS2 Heinrich Events, *Glob. and Plan. Change* 54, 225–238.

Junttila, J. S. A. Sørensen, K. Husum, and M. Hald (2010), Late Glacial-Holocene clay minerals elucidating
glacial history in the SW Barents Sea. *Mar. Geol.* 2010, 276 (1-4), 71–85.
doi:10.1016/j.margeo.2010.07.009.

Kempema, E. W., E. Reimnitz, and P. W. Barnes (1989), Sea ice sediment entrainment and rafting in the Arctic,
J. Sediment. Petrol., 59, 308–317, 1989.

King, E. L., H. Haflidason, H. P. Sejrup, and R. Løvlie, (1998), Glacigenic debris flows on the North Sea Trough
Mouth Fan during ice stream maxima, *Mar. Geol.* 152, 217–246.

Kissel, C., C. Laj, B., Lehman, L. Labyrie, and V. Bout-Roumazeilles, (1997), Changes in the strength of the
Iceland–Scotland Overflow Water in the last 200,000 years: Evidence from magnetic anisotropy
analysis of core SU90-33, *Earth and Plan. Sci. Lett.* 152, 25–36.

Kissel C., C. Laj, L. Labeyrie, T. M. Dokken, A. Voelker, and D. Blamart (1999), Rapid climatic variations
during marine isotopic stage 3: magnetic analysis of sediments from Nordic Seas and North Atlantic.
Earth and Plan. Sci. Lett. 171, 489–502.

Knies, J., C. Vogt, and R. Stein, (1999), Late Quaternary growth and decay of the Svalbard/Barents Sea ice sheet
and paleoceanographic evolution in the adjacent Arctic Ocean, *Geo-Mar. Lett.* 18, 195–202.

Koç-Karpuz, N., and E. Jansen (1992), A High-Resolution Diatom Record of the Last Deglaciation from the SE
Norwegian Sea: Documentation of Rapid Climatic Changes. *Paleoceanography* 7(4), 499–520.

Knutz, P. C., E. J. W. Jones, W. E. N. Austin, and T. C. E. Van Weering (2002a), Glacimarine slope
sedimentation, contourite drifts and bottom current pathways on the Barra Fan, UK North Atlantic
Margin, *Mar. Geol.*188, 129–146.

Knutz, P. C., I. R. Hall, R. Zahn, T. L. Rasmussen, A. Kuipers, M. Moros, and N. J. Shackleton (2002b), Multidecadal ocean variability and NW European ice sheet surges during the last deglaciation, *Geochem., Geophys., Geosyst.* 3, 1077.

Kuipers, A., B. Hansen, V. Hühnerbach, B. Larsen, T. Nielsen and F. Werner (2002), Norwegian Sea overflow through the Faeroe–Shetland gateway as documented by its bedforms, *Mar. Geol.* 188, 147–164.

Laberg, J. S., and T. O. Vorren, (1995), Late Weichselian submarine debris flow deposits on the Bear Island Trough Mouth Fan, *Mar. Geol.* 127, 45–72.

Landvik, J. Y., S. Bondevik, A. Elverhøi, W. Fjeldskaar, J. Mangerud, O. Salvigsen, J. M. Siegert, J. I. Svendsen, and T. O. Vorren (1998), The last glacial maximum of Svalbard and the Barents Sea area: Ice sheet extent and configuration. *Quaternary Sci. Rev.* 17 (1-3), 43-75.

Landvik, J. Y., Ó. Ingólfsson, J. Mienert, S. J. Lehman, A. Solheim, A. Elverhøi, and D. Ottesen (2005), Rethinking Late Weichselian ice-sheet dynamics in coastal NW Svalbard. *Boreas* 34, 7–24.

Landvik, J., E. J. Brook, L. Gualtieri, H. Linge, G. Raisbeck, O. Salvigsen, and F. Yiou (2013), [10]Be exposure age constraints on the Late Weichselian ice sheet geometry and dynamics in inter ice-stream areas, western Svalbard. *Boreas* 42, 43–56.

Landvik, J. I., H. Alexanderson, M. Henriksen, and Ó. Ingólfsson (2014), Landscape imprints of changing glacial regimes during ice-sheet build-up and decay: a conseptual model from Svalbard, *Quaternary Sci. Rev.* 92, 258–268.

Laskar, J., P. Robutel, F. Joutel, M. Gastineau, A. C. M. Correira, and B. Levrard (2004), A long-term numerical solution for the insolation quantities of the Earth. *Astron. Astrophys.* 428, 261–285.

Lubinski, D., S. Korsun, L. Polyak, S. L. Forman, S. J. Lehman, F. A. Herlihy, and G. M. Miller (1996), The last deglaciation of the Franz Victoria Trough, Northern Barents Sea, *Boreas* 25, 89–100.

Lucchi, R. G., A. Camerlenghi, M. Rebesco, E. Colmenero-Hidalgo, F. J. Siero, L. Sagnotti, R. Urgeles, R. Melis, C. Morigi, M.-A. Bárcena, G. Giorgetti, G. Villa, D. Persico, J.-A. Flores, A. S. Rigual-Hernandez, M. T. Pedrosa, P. Macri, and A. Caburlotto (2013), Postglacial sedimentary processes on the Storfjorden and Kveithola trough mouth fans: Significance of extreme glacimarine sedimentation, *Glob. and Plan. change* 111, 309–326.

Lundqvist, J., (1986), Late weichselian glaciation and deglaciation in Scandinavia, *Quaternary Sci. Rev.* 5, 269–192

MacAyeal, D. R. (1993a), Binge/purge oscillations of the Laurentide Ice Sheet as a cause of the North Atlantic's Heinrich events, *Paleoceanography* 8(6), 775–784, doi: 10.1029/93PA02200

MacAyeal, D. R. (1993b), A low-order model of the Heinrich Event Cycle, *Paleoceanography* 8(6), 767–773, doi: 10.1029/93PA02201

Mangerud, J. (2004), Ice sheet limits in Norway and on the Norwegian continental shelf, *In* Ehlers, J., and P. L. Gibbard (eds.), Quaternary Glaciations – Extent and Chronology: Part I: Europe, Elsevier, Amsterdam, 271–284.

Mangerud, J., T. Dokken. D. Hebbeln, B. Heggen, Ó. Ingólfsson, J.Y. Landvik, V. Mejdahl, J. I. Svendsen, and T. O. Vorren (1998), Fluctuations of the Svalbard-Barents Sea Ice Sheet during the last 150 000 years, *Quaternary Sci. Rev.* 17(1-3), 11–42.

Matsumoto, K. (1996), An iceberg drift and decay model to compute the ice-rafted and iceberg meltwater flux: Application to the interglacial North Atlantic. *Paleoceanography* 11(6), 729–742.

Marcott, S. A., P. U. Clark, L. Padman, G. P. Klikhammer, S. R. Springer, Z. Liu, B. L. Otto-Bliesner, A. E. Carlson, A. Ungerer, J. Padman, F. He, J. Cheng, and A. Schmittner (2011), Ice-shelf collapse from subsurface warming as a trigger for Heinrich events, PNAS, doi:10.1073/pnas.1104772108.

Marnela, M., B. Rudels, K. A. Olsson, L. G. Anderson, E. Jeansson, D. J. Torres, M.-J. Messias, J. H. Swift, and A. J. Watson (2008), Transports of Nordic Seas water masses and excess SF6 through Fram Strait to the Arctic Ocean. *Progr. in Oceanogr.* 78, 1-11.

McCave, I. N., and I. R. Hall (2006), Size sorting in marine muds: Processes, pitfalls, and prospects for paleoflow-speed proxies, *Geochem. Geophys. Geosys.* 7, Q10N05, doi:10.1029/2006GC001284.

McCave, I. N., B. Manighetti, N. A. S. Beveridge (1995), Circulation in the glacial North Atlantic inferred from grain-size measurements, *Nature* 374, 149–152.

Moros, M., R. Endler, K. S., Lackschewitz, H.-J. Wallrabe-Adams, J. Mienert, and W. Lemke (1997), Physical properties of Reykjanes Ridge sediments and their linkage to high-resolution Greenland Ice Sheet Project 2 ice core data, *Paleoceanography* 12(5) 687–695.

Moros, M., A. Kuijpers, I., Snowball, S. Lassen, D. Bäckström, F. Gingele, J. McManus (2002), Were Glacial Iceberg Surges in the North Atlantic triggered by Climatic Warming?, *Mar. Geol.* 192, 393–417.

Moros, M., J. F. McManus, T. Rasmussen, A. Kuipers, T. Dokken, I. Snowball, T. Nielsen, and E. Jansen (2004), Quartz content and the quartz-to-plagioclase ratio determined by X-ray diffraction: a proxy for ice rafting in the northern North Atlantic? *Earth and Plan. Sci. Lett.* 218, 389–401.

Müller, A., and J. Knies (2014), Trace elements and cathodolominisence of detrital quartz in Arctic marine sediments – a new ice rafed debris provenance study, *Clim. Past.* 9, 2615–2630.

Nees, S., A. V. Altenbach, H. Kassens and J. Thiede (1997), High-resolution record of foraminiferal response to late Quaternary sea-ice retreat in the Norwegian-Greenland Sea, *Geology* 25(7), 659–662.

Naugthon, F., M. F. Sánchez Goñi, S. Desprat, J.-L. Turon, J. Duprat, B. Malaizé, C. Joli, E. Cortijo, T. Drago, and M. C. Freitas (2007), Present-day and past (last 25 000 years) marine pollen signal off western Iberia, *Mar. Michopal.* 62, 91–114.

Naugthon, F., M. F. Sánchez Goñi, M. Kageyama, E. Bard, J. Duprat, E. Cotijo, S. Desprat, B. Malaizé, C. Joly, F. Rostek, and J.-L. Turon (2009), Wet to dry climatic trend in north-western Iberian within Heinrich events, *Earth and Pla. Sci. Lett.* 284, 329–342.

Nørgaard-Pedersen, N., R. F. Spielhagen, H. Erlenkeuser, P. M. Grootes, J. Heinemeier, and J. Knies, (2003), Arctic Ocean during the Last Glacial Maximum: Atlantic and polar domains of surface water mass distribution and ice cover, *Paleoceanography* 18 (3), PA1063, doi:10.1029/2002PA000781.

Osiński, R., P. Wieczorek, A. Beszczyńska-Möller, and I. Goszczko (2003), ADCP-referenced geostrophic velocity and transport in the West Spitsbergen Current, *Oceanologia* 45 (3), 425–435.

Ottesen, D., J. A. Dowdeswell, and L. Rise (2005), Submarine landforms and the reconstruction of fast-flowing ice streams within a large Quaternary ice sheet: the 2,500 km-long Norwegian-Svalbard margin (57° to 80°N). *Geological Society of America, Bulletins* 117, 1033–1050.

Ottesen, D., J. A. Dowdeswell, J. Y. Landvik, and J. Mienert (2007), Dynamics of the Late Weichselian ice sheet on Svalbard inferred from high-resolution sea-floor morphology, *Boreas* 36(3), 286–306.

Owen, M., S. Day, and M. Maslin (2007), Late Pleistocene submarine mass movements: occurrence and causes. *Quaternary Sci. Rev.* 26 (7-8), 958–978.

Pedrosa, M., A. Camerlenghi, B. De Mol, R. Urgeles, M. Rebesco, R. G. Lucchi and Shipboard participants of the SVAIS and EGLACOM Cruises (2011). Seabed Morphology and Shallow Sedimentary Structure of the Storfjorden and Kveithola Trough-Mouth Fans (north west Barents Sea), *Mar. Geol.*, 286(1-4), 65-81. doi:10.1016/j.margeo.2011.05.009

Polyak, L., F. Niessen, V. Gataullin, and V. Gainanov (2008), The eastern extent of the Barents-Kara ice sheet during the Last Glacial Maximum based on seismic-reflection data from the eastern Kara Sea, *Pol Res.* 27, 162–174.

Praetorius, S. K., J. F. McManus, D. W. Oppo, and W. B. Curry (2008), Episodic reductions in bottom-water currents since the last ice age, *Nature Geoscience* 1, 449-452 doi:10.1038/ngeo227.

Pudsey, C.J., and J. Evans (2001), First survey of Antarctic sub-ice shelf sediments reveals mid-Holocene ice shelf retreat, *Geology* 29, 787–790.

Quadfasel, D., J. C. Gascard, and K. P. Koltermann (1987), Large-Scale Oceanography in Fram Strait During the 1984 Marginal Ice Zone Experiment, *J. Geophys. Res.* 92 (C7), 6719–6728.

Radhakrishnamurty, C., S. D. Likhite, B. S Amin, and B. L. K Somayayulu (1968), Magnetic susceptibility stratigraphy in ocean sediment cores, *Earth and Plan. Sci. Lett.* 4, 464–468.

Rasmussen, T. L., and E. Thomsen (2013), Pink marine sediments reveal rapid ice melt and Arctic meltwater discharge during Dansgaard-Oeschger warmings, *Nature Communications.* DOI: 10.1038/ncomms3849

Rasmussen, T.L., and E. Thomsen (2015). Paleoceanographic development in Storfjorden, Svalbard, during the deglaciation and Holocene: evidence from benthic foraminiferal records, *Boreas* 44, 24–44.

Rasmussen, T.L., E. Thomsen, T. C. E. van Weering, and L. Labeyrie (1996a), Rapid changes in surface and deep water conditions at the Faroe margin during the last 58,000 years, *Paleoceanography* 11(6), 757–771.

Rasmussen, T. L., T. E. van Weering, and L. Labeyrie (1996b). High resolution stratigraphy of the Faeroe-Shetland Channel and its relation to North Atlantic paleoceanography: the last 87 kyr. *Mar. Geol.* 131, 75–88.

Rasmussen, T. L., E. Thomsen, and T. C. E. van Weering, (1998), Cyclic changes in sedimentation on the Faeroe Drift 53-9 kyr BP related to climate variations. *In,* Stoker, M., D. Evans, and R. Cramp (eds), Geological Processes on Continental Margins: Sedimentation, Mass-Wasting and Stability. Geological Society, *London, Special Publications* 129, 255–267.

Rasmussen, T. L., E. Thomsen, and T. Nielsen, (2014), Water mass exchange between the Nordic Seas and the Arctic Ocean on millennial time scale during MIS 4–2. *Geochem. Geophys. Geosys.* 15. 530–544. doi: 10.1002/2013GC005020.

Reimer, P. J., B. Edouard, A. Bayliss, J. W. Beck, P. G. Blackwell, C. B. Ramsey, C. E. Buck, H. Cheng, R. L. Edwards, M. Friedrich, P. M. Grootes, T. P. Guilderson, H. Haflidason, I. Hajdas, C. Hatté, T. J. Heaton, D. L. Hoffmann, A. G. Hogg, K. A. Hughen, K. F. Kaiser, B. Kromer, S. W. Manning, M. Nju, R. W. Reimer, D. A. Richards, E. M. Scott, J. R. Southon, R. A. Staff, C. S. M. Turney, and J. van der Plicht (2013), INTCAL13 and Marine13 radiocarbon age calibration curves 0–50,000 years cal BP, *Radiocarbon* 55, 1869–1886.

Robinson, S. G., and I. N. McCave (1994), Orbital forcing of bottom current enhanced sedimentation on Feni Drift, NE Atlantic, during the mid-Pleistocene, *Paleoceanography* 9, 943–972.

Robinson, S., M. Maslin, and I. McCave (1995), Magnetic Susceptibility Variations in Upper Pleistocene Deep-Sea Sediments of the NE Atlantic: Implications for Ice Rafting and Paleocirculation at the Last Glacial

Maximum, *Paleoceanography* 10 (2), 221–250.

Ruddiman, W. F. (1977), Late Quaternary deposition of ice-rafted sand in sub-polar North Atlantic (40-60 N), *Geological Society of America, Bull*etins 88, 1813–1827.

Ruddiman, W. F., and A. McIntyre (1981), Ocean Mechanisms for Amplification of the 23,000-Year Ice-Volume Cycle, *Science* 212, 617–627.

Rudels, B. (1987), On the mass balance of the Polar Ocean, with special emphasis on the Fram Strait. *Norw. Polar Inst. Skr.* 188, 53.

Rudels, B., R. Meyer, E. Fahrbach, V. V. Ivanov, S. Østerhus, D. Quadfasel, U. Schauer, V. Tverberg, and R. A. Woodgate (2000), Water mass distribution in Fram Strait and over the Yermak Plateau in summer 1997. *Ann. Geophys.*18, 687–705.

Russel-Head, D. D. (1980), Melting of free-drifting icebergs, *Ann. Glaciol.* 1, 119–122.

Rüther, D. C., R. Mattingsdal, K. Andreassen, M. Forwick, and K. Husum (2011), Seismic architecture and sedimentology of major grounding zone system deposited by the Bjørnøya Ice Stream during Late Weichselian deglaciation, *Quaternary Sci. Rew.* 30, 2776–2792.

Rørvik, K.-L., J. S. Laberg, M. Hald, E. K. Ravna, and T. O. Vorren (2010), Behavior of the northwestern part of the Fennoscandian Ice Sheet during the Last Glacial Maximum – a response to external forcing. *Quaternary Sci. Rew.* 29, 2224–2237.

Shaffer, G., S. M. Olsen, and C. J. Bjerrum (2004), Ocean subsurface warming as a mechanism for coupling Dansgaard-Oeschger climate cycles and ice-rafting events, *Geophys. Res. Lett.* 31, L24202, doi:10.1029/2004GL020968

Shauer, U., E. Fahrbach, S. Østerhus, and G. Rohardt (2004), Arctic warming through the Fram Strait: Oceanic heat transport from 3 years of measurements. *J. Geophys. Res.*109, C06026, doi:10.1029/2003JC001823

Smythe, F. W., W. F. Ruddiman, and.D. N. Lumsden (1985), Ice-rafted evidence of long-term North Atlantic Circulation, *Mar. geol.* 64 131–141

Siegert, M. J., and J. A. Dowdeswell, (1995a), Modelling Ice sheet sensitivity to Late Weichselian environments in the Svalbard-Barents Sea region, *J. Quaternary Sci.* 10 (1), 33–43.

Siegert, M. J., and J. A. Dowdeswell, (1995b), Numerical Modeling of the Late Weichselian Svalbard-Barents Sea Ice Sheet, *Quaternary Res.* 43, 1–13.

Siegert, M. J., and J. A. Dowdeswell, (2002). Late Weichselian iceberg, surface-melt and sediment production from the Eurasian Ice Sheet: results from numerical ice-sheet modelling, *Mar. Geol.* 1988, 109–127.

Siegert, M. J., and J. A. Dowdeswell, (2004), Numerical reconstructions of the Eurasian Ice Sheet and climate during the Late Weichselian, *Quaternary Sci. Rev.* 23 (11-13), 1273–1283.

Solheim, A., J. I. Faleide, E. S. Andersen, A. Elverhøi, C. F. Forsberg, K. Vanneste, G. Uenzelmann-Neben, and J. E. T. Channell (1998). Late cenozoic seismic stratigraphy and glacial geological development of the East Greenland and Svalbard-Barents Sea continental margins. *Quaternary Sci. Rev.* 17 (1-3), 155–184.

Skirbekk, K., D. Klitgaard Kristensen, T. L. Rasmussen, N. Koç, and M. Forwick, (2010), Holocene climate variations at the entrance to a warm Arctic fjord: Evidence from Kongsfjorden through, Svalbard. In Howe, J. A., W. E. N. Austin, M. Forwick , and M. Paetzel (eds.), Fjord Systems and Archives, Geological Society, *London, Special Publications* 344, 291–306.

Ślubowska, M. A., N. Koç, T. L. Rasmussen, and D. Klitgaard-Kristensen (2005), Changes in the flow of Atlantic water into the Arctic Ocean since the last deglaciation: Evidence from the northern Svalbard continental margin, 80°N. *Paleoceanography* 20, PA4014, doi:10.1029/2005PA001141.

Ślubowska-Woldengen, M., T. L. Rasmussen, N. Koç, D. Klitgaard-Kristensen, F. Nilsen, and A. Solheim, (2007), Advection of Atlantic Water to the western and northern Svalbard shelf since 17,500 cal yr BP. *Quaternary Sci. Rev.* 26 (3-4), 463–478.

Stabell, B. (1986), A diatom maximum horizon in upper quaternary deposits. *Geolog. Rundschau* 75 (1), 175–184.

Stanford, J. D., E. J. Rohling, S. E. Hunter, A. P. Roberts, S. O. Rasmussen, E. Bard, J. McManus, and R. G. Fairbanks (2006), Timing of meltwater pulse 1a and climate respomses to meltwater injections, *Paleoceanography* 21(4), PA4103, doi:10.1029/2006PA001340.

Svendsen, J. I., and J. Mangerud (1997), Holocene glacial and climatic variations on Spitsbergen, Svalbard, *The Holocene* 7 (1), 45–57, doi:10.1177/095968369700700105.

Svendsen, J. I., H. Alexanderson, V. Astakhov, J. Demidov, J. A. Dowdeswell, M. Henriksen, C. Hjort, M. Houmark-Nielsen, H. Hubberten, Ó. Ingólfsson, M. Jakobsson, K. Kjær, E. Larsen, H. Lokrantz, E. P. Luunka, A. Lyså, J. Mangerud, O. Maslenikova, A. Matioushkov, A. Murray, P. Möller, F. Niessen, M. Saarnisto, M. Siegert, R. Stein, and R. Spielhagen (2004), Ice sheet history of northern Eurasia. *Quaternary Sci. Rev. 22,* 1229–1271.

Stickley, K. E., K. St John, N. Koc, R. W. Jordan, S. Passchier, R. B. Pearce, and L. E. Kerns (2009), Evidence for middle Eocene Arctic sea ice from diatoms and ice-rafted debris, *Nature* 460, 376–379.

Stuiver, M., and P. Reimer (1993), Extended ^{14}C database and revised Calib 3.0 age calibration program. *Radiocarbon* 35, 215–230.

Sztybor, K., C. Consolaro, T.L. Rasmussen, S. Bünz, J. Mienert, (2012), Methane release from the seabed and climate change. Arctic Frontiers 2012, Energies of the High North, Jan. 25-27, Tromsø, Norway, Book of Abstracts, p. 146.

Thornalley, D. J. R., S. Barker, J. Becker, I. R. Hall, G. Knorr (2013), Abrupt changes in deep Atlantic circulation during the transition to full glacial conditions. *Paleoceanography* 28, 253–262.

van Kreveld, S., M. Sarnthein, H. Erlenkeuser, P. Grootes, S. Jung, S., M. J. Nadeau, U. Pflaumann, and A. Voelker (2000), Potential links between surging ice sheets, circulation changes, and the Dansgaard-Oeschger cycles in the Irminger Sea 60-18 kyr, *Paleoceanogrphy* 15 (4), 425–442.

Vogt, C., and J. Knies (2008), Sediment dynamics in the Eurasian Arctic Ocean during the last deglaciation — the clay mineral group smectite perspective, *Mar. geol.* 250(3–4) 211–222.

Vogt, C., and J. Knies (2009), Sediment pathways in the western Barents Sea inferred from clay mineral assemblages in surface sediments, *Norw. J. Geol.* 89(1-2), 41-55.

Vogt, C., J. Knies, R. F. Spielhagen, and R. Stein (2001), Detailed mineralogical evidence for two nearly identical glacial/deglacial cycles and Atlantic water advection to the Arctic Ocean during the last 90,000 years, *Glob. and Plan. Change 31,* 23–44.

Vorren, T. O., and J. S. Laberg (1997), Through mouth fans – Paleoclimate and ice-sheet monitors. *Quaternary Sci. Rev.* 16 (8), 865–881.

Vorren, T. O., J. S. Laberg, F. Blaume, J. A. Dowdeswell, N. H. Kenyon, J. Mienert, J. Rumour, and F. Werner (1998), The Norwegian-Greenland Sea continental margins: Morphology and late quaternary sedimentary processes and environments, *Quaternary Sci. Rev.* 17 (1-3), 273–302.

Walczowski, W., J. Piechura R. Osiński, and P. Wieczorek (2005), The West Spitsbergen Current volume and heat transport from synoptic observations in summer, *Deep-Sea Res. I* 52,1374–1391.

Watkins, N. D., J. Keany, M. T. Ledbeiter, and T. C. Huang (1974), Antarctic glacial history from analysis of ice rafted deposits in marine sediments: new model and initial tests, *Science* 186, 533–536

Weltje, G. J., and M. A. Prins (2003), Muddled or mixed? Inferring paleoclimate from size distribution of deep-sea clastics, *Sediment. Geol.* 162, 39–62.

Weltje, G. J., and M. A. Prins (2007), Genetically meaningful decomposition of grain-size distributions, *Sediment. Geol.* 202, 409–424.

Werner, K., R. F. Spielhagen, D. Bauch, H. C. Hass, and E. Kandiano (2013), Atlantic Water advection versus sea-ice advances in the eastern Fram Strait during the last 9 ka – multi proxy evidence for a two-phase Holocene, *Paleoceanography* 28, 283–295.

Winsborrow, M. C. M., K. Andreassen, G. D. Corner, and J. S. Laberg (2010), Deglaciation of a marine-based ice sheet: Late Weichselian paleo-ice dynamics and retreat in the southern Barents Sea reconstructed from onshore and offshore glacial geomorphology, *Quaternary Sci. Rev.* 29, 424–442.

Zamelczyk, K., T. L. Rasmussen, K. Husum, F. Gotliebsen, and M. Hald (2014), Surface water conditions and carbonate preservation in the Fram Strait during marine isotope stage 2, 28.8–15.4 kyr, *Paleoceanography* 29, 1–12, doi:10.1002/2012PA002448.

Figures

Captions

Figure 1. Study area and location of investigated cores in **a)** 2D view (modified from Paper I) and **b)** 3D view. Cores investigated in Paper II, III and IV are marked by red stars. Green star mark the core JM05-031GC to which the cores JM04-025PC and JM03-374PC are correlated in Papers II and III. Black dots mark cores that are included in Paper I only.

Figure 2. **a)** Ice melting as a function of temperature and the effect in the melting capacity of water by a warming of 3K from the initial temperature (e.g., from -1.5 to +1.5 °C). **b)** Parameters affecting IRD-flux and IRD concentration) **c-d)** Parameters affecting the relative abundance of local (c) and allochthonous (d) IRD, + and - indicates if a correlation is positive or negative.

Figure 3. a-c) Scatter plots and regression analyses of IRD counts and the wt% of the same fractions in the core JM03-373PC.

Figure 4. a-c) Scatter plots and regression analyses of IRD counts in different gran.size fractions in the core JM03-374PC. **d)** Percentage of mono-crystalline quartz in the grain-size fractions 150–250 μm and 250–500 μm in core JM03-374PC. **e)** Scatter plot and regression analysis of the two quartz percentage data series in panel d.

Figure 5. Normalized magnetic susceptibility (Norm. MS) from 11 cores from the western Svalbard slope (76° 13' to 79° 37' N) stacked into one record based on MS and lithology. Absolute ages can be extracted from the Tie-points of the stacked record. Tie-Point 6.1 (in grey) is from Paper III, other Tie-Points from Paper I. Original AMS[14]C dates as presented in Paper I corrected for 440 yr reservoir effect in *cursive*. Calendar ages are calibrated using calib 7.02 and the Marine13 data set (Stuiver and Reimer, 1993; Reimer et al., 2013) with Δr of 0 (data from Paper I, Figure 4). All ages are presented with one standard deviation uncertainty.
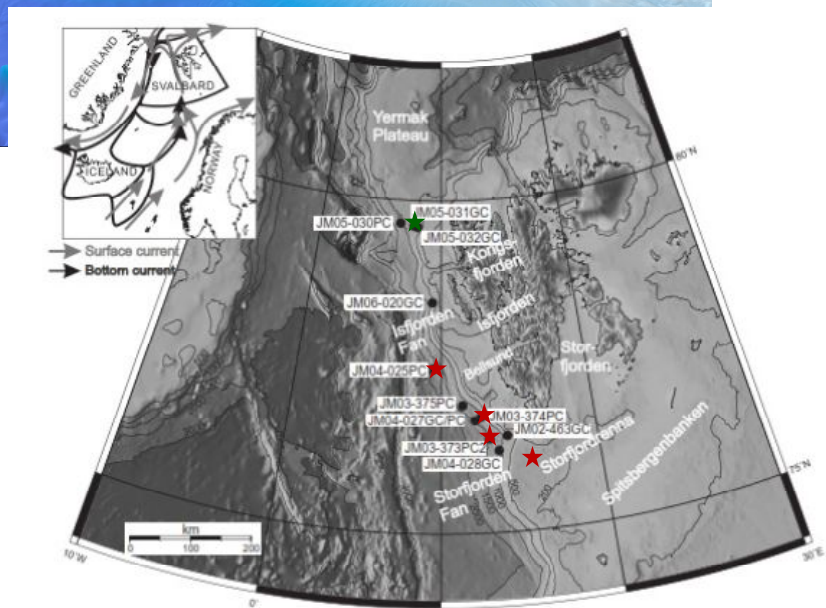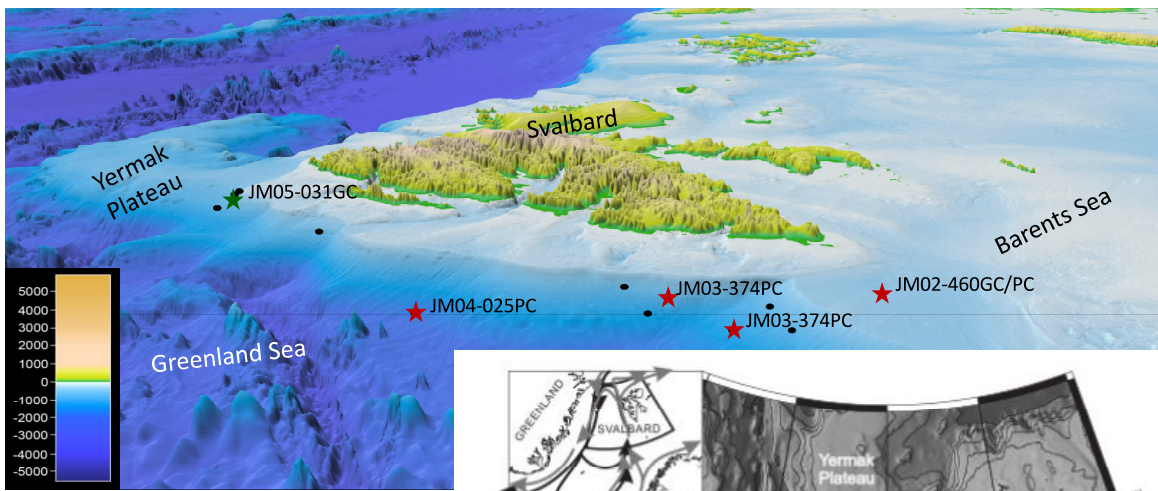
Figure 1

a

b

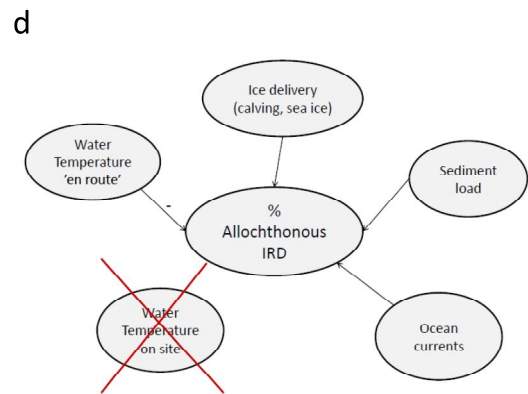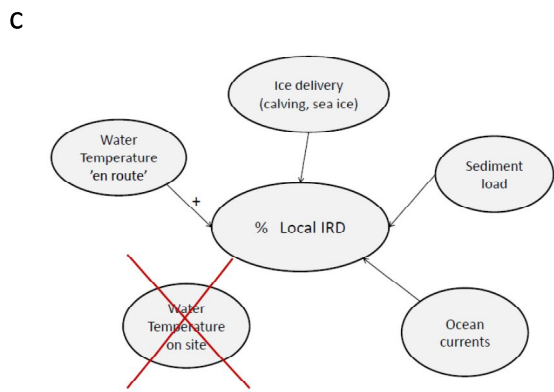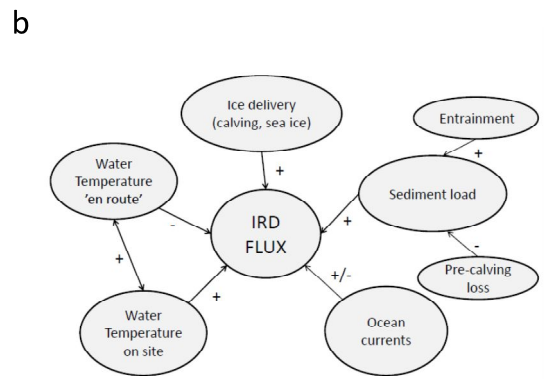c

d
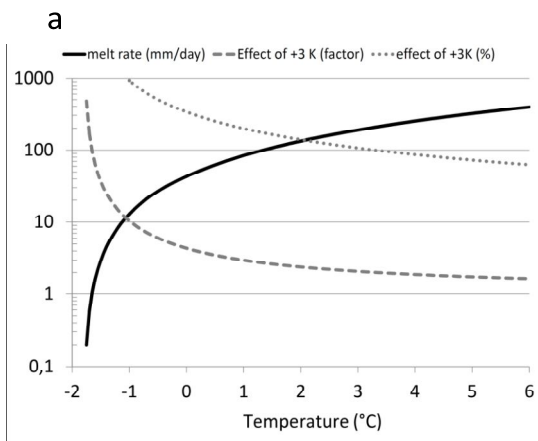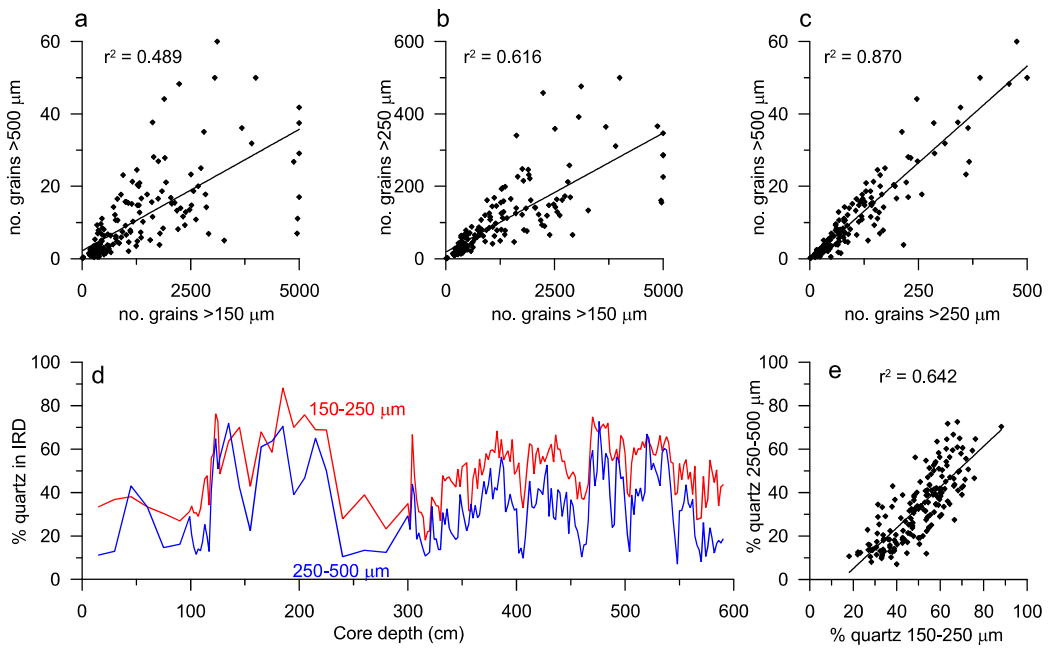
Figure 2

Figure 3

Figure 4

Norm. MS (σ)

TP1 — 7.53 ±0.06 ¹⁴C kyr BP
8.44 ±0.06 ka

TP2 — 8.80 ±0.10 ¹⁴C kyr BP
9.97 ±0.14 ka

TP3 — 8.95 ±0.10 ¹⁴C kyr BP
10.22 ±0.14 ka

TP4 — 12.25 ±0.15 ¹⁴C kyr BP
14.42 ±0.28 ka

TP5 — 12.40 ±0.15 ¹⁴C kyr BP
14.60 ±0.27 ka

TP6 — 12.70 ±0.15 ¹⁴C kyr BP
15.07 ±0.31 ka

TP6.1 — 16.67 ±0.12 ¹⁴C kyr BP
20.17 ±0.17 ka

TP7 — 19.70 ±0.13 ¹⁴C kyr BP
23.77 ±0.17 ka

TP8 — 20.14 ±0.13 ¹⁴C kyr BP
24.24 ±0.17 ka

TP9 — 22.80 ±0.20 ¹⁴C kyr BP
27.18 ±0.20 ka

Depth (cm)

Figure 5